

**Universität für Bodenkultur Wien**

University of Natural Resources and Life Sciences, Vienna



Department of Water, Atmosphere and Environment  
Institute of Hydrology and Water Management (HyWa)



## **MASTERARBEIT / MASTER'S THESIS**

### TEMPERATURE ANOMALIES OF ALPINE LAKES IN THE LOWER TAUERN REGION

verfasst von / submitted by

Steffen Büchen, B.Sc.

angestrebter akademischer Grad /  
in partial fulfilment of the requirements for the degree of

Diplomingenieur (Dipl.-Ing.)

Wien, 2020 / Vienna, 2020

Matrikelnummer / registration number	01240674
Studienkennzahl / ID of study programme	UH 066 447
Studienbezeichnung / name of study programme	Water Management and Environmental Engineering
Betreuer / supervisors	Karsten Schulz, Univ.Prof. Dipl.Geoökol. Dr.rer.nat. Mathew Herrnegger, Dipl.-Ing. Dr.nat.techn.



# Abstract

From July 1998 to September 2003 the lake surface water temperature of alpine lakes in the Niederen Tauern region was continually measured by data loggers. Anomalies were found in the evaluation of the collected data, as there were significant differences in the surface water temperature characteristics of similarly shaped lakes at comparable altitudes. These temperature differences were already investigated in a previous study, which examined several influencing factors and suspects that comparatively colder lakes are affected by inflowing meltwater.

Since no definitive cause for the temperature differences was found in the previous study, and some of the lakes are now subject of a new research project (CLAIMES), the data will be examined again in this work. This thesis is intended to form the basis for an initial assessment of the lakes hydrological conditions and attempts to identify the causes of the anomalies in the lakes' summer water temperature by using approaches that are as straightforward as possible. The first approach is therefore limited to a terrain model of the catchments and the associated lapse rate of the air temperature together with the assumption that water temperature is related to air temperature. In the following steps meteorological information from the SPARTACUS data set of ZAMG will be integrated, which relies on spatial interpolation of station observations. For the second approach, the terrain model will be supplemented by air temperature data to find out whether there is a correlation between air and water temperature at catchment level. The third approach then aims at representing the energy input in the catchment areas by further including precipitation data and comparing it to the water temperature.

The results of the first approach do not indicate, that the lakes different water temperatures can be solely explained by means of proportions of altitude zones and therefore air temperature lapse rate alone. Approach two, assuming a relationship between the lake water and air temperature lapse rates, cannot be confirmed either. Where comparable studies show a correlation of lapse rates during the summer months, in this study the lapse rate of the air temperature shows a different distribution and average gradient compared to the water temperature. For the third approach, the general energy input shows a tendency for warm lakes to be supplied with more energy in the summer than cold classified lakes, although it is has not become clear whether the high input is due to the air temperature or precipitation. Concerning the months from September to May, a higher absolute energy input on days with air temperature below 0 °C can be observed for the cold classified lakes.

These indications suggest that the influence of snowmelt might possibly be the biggest contributor to the fluctuation of water temperature between the lakes, which was already noted in the first study. In conclusion, however, this work cannot provide final proof of this.



# Kurzfassung

Von Juli 1998 bis September 2003 wurde die Seewassertemperatur von Alpenseen in den Niederen Tauern kontinuierlich mit Datenloggern gemessen. Bei der Auswertung der gesammelten Daten wurden Anomalien festgestellt, da es signifikante Unterschiede in der Charakteristik der Oberflächenwassertemperatur von ähnlich geformten Seen in vergleichbaren Höhenlagen gab. Diese Temperaturunterschiede wurden bereits in einer früheren Studie untersucht, die mehrere Einflussfaktoren untersuchte und vermutet, dass die vergleichsweise kälteren Seen durch Schmelzwasser beeinflusst werden.

Da in der vorherigen Studie keine endgültige Ursache für die Temperaturunterschiede gefunden wurde und einige der Seen nun Gegenstand des CLAIMES-Projektes sind, werden die Daten in dieser Arbeit erneut untersucht. Diese Arbeit soll eine erste Einschätzung der hydrologischen Bedingungen der Seen bilden und versucht, die Ursachen für die Anomalien der Sommer-Wassertemperatur der Seen mit möglichst einfachen Ansätzen zu identifizieren. Der erste Ansatz beschränkt sich auf ein Geländemodell der Einzugsgebiete und geht davon aus, dass deren Morphologie zusammen mit der Lufttemperatur lapse rate einen ersten Hinweis auf die Anomalien geben kann. In den folgenden Schritten werden räumlich interpolierte meteorologische Daten aus dem SPARTACUS-Datensatz verwendet. Für den zweiten Ansatz wird das Geländemodell durch Lufttemperaturdaten ergänzt, um herauszufinden, ob auf Einzugsgebiets-Ebene ein Zusammenhang zwischen Luft- und Wassertemperatur besteht. Der dritte Ansatz zielt anschließend darauf ab den Energieeintrag in den Einzugsgebieten nachzubilden und mit der Wassertemperatur zu vergleichen, indem auch Niederschlagsdaten mit einbezogen werden.

Die Ergebnisse des ersten Ansatzes zeigen, dass die unterschiedlichen Wassertemperaturen der Seen nicht allein durch die Topographie und lapse rate der Lufttemperatur erklärt werden können. Auch der zweite Ansatz, der eine Beziehung zwischen der Wasser- und der Lufttemperatur lapse rate annimmt, kann nicht bestätigt werden. Wo vergleichbare Studien eine Korrelation beider lapse rate während der Sommermonate zeigen, zeigt in dieser Studie die der Lufttemperatur eine andere Verteilung und einen anderen durchschnittlichen Gradienten als die Wassertemperatur. Für den dritten Ansatz zeigt der allgemeine Energieeintrag eine Tendenz, dass warme Seen im Sommer mit mehr Energie versorgt werden als kalt klassifizierte Seen, wobei nicht klar ist, ob der hohe Eintrag auf die Lufttemperatur oder auf den Niederschlag zurückzuführen ist. Gemittelt über die Monate September bis Mai ist bei den kalt klassifizierten Seen ein höherer absoluter Energieeintrag an Tagen mit einer Lufttemperatur unter 0 °C zu beobachten.

Diese Hinweise deuten darauf hin, dass der Einfluss der Schneeschmelze möglicherweise den größten Beitrag zur Schwankung der Wassertemperatur zwischen den Seen leistet, was bereits in der ersten Studie festgestellt wurde. Zusammenfassend kann diese Arbeit jedoch keinen endgültigen Beweis dafür liefern.

# Affirmation

I declare on my honour that I have written this work independently and without outside help, that I have not used sources other than those indicated, and that I have marked as such the places taken literally or in terms of content from the sources used.

# Abbreviations

CLAIMES	CLimate response of Alplne lakes: resistance variability and Management consequences for Ecosystem Services
CLC	CORINE Land Cover
DEM	Digital Elevation Model
GB	Gigabyte
GIS	Geographic Information System
GPS	Global positioning system
JJA	June July August
LiDAR	Light Detection And Ranging
LSWT	Lake Surface Water Temperature
m a.s.l.	Meter above sea level
MB	Megabyte
RMSE	Root-mean-square deviation
SPARTACUS	Spatiotemporal reanalysis dataset for climate in Austria
T <sub>n</sub>	Minimum temperature
T <sub>x</sub>	Maximum temperature
ZAMG	Zentralanstalt für Meteorologie und Geodynamik



# Contents

<b>1</b>	<b>Introduction</b>	<b>1</b>
1.1	Limnologic aspects . . . . .	2
1.2	Modelling types . . . . .	6
1.3	Aim of the thesis . . . . .	11
<b>2</b>	<b>Data description</b>	<b>14</b>
2.1	Study area . . . . .	14
2.2	Lake water temperature . . . . .	17
2.3	Elevation data . . . . .	19
2.4	Temperature and precipitation data . . . . .	19
<b>3</b>	<b>Methods</b>	<b>21</b>
3.1	Data preparation . . . . .	21
3.2	Lake temperature classification . . . . .	24
3.3	Approaches . . . . .	26
<b>4</b>	<b>Results and discussion</b>	<b>30</b>
4.1	Approach I – Catchment topography . . . . .	30
4.2	Approach II – Catchment air temperature . . . . .	37
4.3	Approach III – Catchment energy input . . . . .	39
<b>5</b>	<b>Conclusion and outlook</b>	<b>44</b>
	<b>Appendices</b>	<b>52</b>
<b>A</b>	<b>Tables</b>	<b>53</b>
<b>B</b>	<b>Figures</b>	<b>59</b>



# 1. Introduction

The intention of this work is to analyze the causes of temperature anomalies in 44 lakes of the Niedere Tauern by means of their catchment topography and hydrological drivers like local air temperature and precipitation.

Of the lakes investigated in this study, 11 are also the subject of the CLAIMES<sup>1</sup> project of the University of Innsbruck, which is investigating whether and what impacts climate change has on alpine lakes and their ecosystem services. Based on the general definition of the ecosystem services in Brondizio et al. (2019) as "nature's contributions to people", the services of those 11 lakes are defined by Fontana et al. (2019) as aesthetic value, their use for outdoor recreation (hiking, swimming, mountain biking, etc.) and their suitability for livestock farming, irrigation, hunting and fishing. Since the water temperature has a major impact on the chemistry and biological communities of a lake, a possible thermal shift due to climate change will be evaluated within the project. As noted above, this work will be focused on the temperature anomalies and the influence of hydrological forces on them, which could not be properly explained in a previous study.

This study by Thompson et al. (2005) was aimed to investigate the lakes' sensitivity to climatic factors and therefore measured their water temperature from July 1998 to September 2003. This study used °C, in order to allow a clearer representation of temperatures below 0 °C, they are converted to K. Anomalies were found in the evaluation of the collected temperature data, as there were significant differences in the surface water temperature characteristics of similarly shaped lakes at comparable altitudes. Where a relationship between altitude and water temperature would normally be expected, the measured data showed clear differences with some lakes being unusually cold and some being significantly warmer than the rest. The authors therefore tried to find reasons for these temperature differences and finally concluded that the comparatively colder lakes are most likely influenced by inflowing meltwater. Using a multivariate analysis, a model for estimating the water temperature of the lakes was set up and it was in this way noted that direct solar radiation has no particular influence on the lakes water temperature. The most important parameters were defined as the southwest and northeast facing shares of the catchment areas, the trophy of the lakes and their area and volume. Furthermore, possible effects of climate change on the lakes were evaluated based on a local warming of 5 to 6 K in summer air temperature, combined with a further 6 K warming caused by the absence of snowpacks within the catchments. Based on these possible changes, the researchers detected that the surface water of the most sensitive lakes will increase by about 12 K in the coming century. However, the lakes can also be indirectly affected if temperature-related factors such as precipitation or snow cover in

---

<sup>1</sup>Climate response of Alpine lakes: resistance variability and Management consequences for Ecosystem Services

the catchment area, which normally contribute to cooling, are changing as well.

Higher water temperature of the lakes caused by global warming would, in terms of ecosystem services, mainly have an impact on their biology. Thus Weckström et al. (2016) have assessed changes of the planktic and benthic communities of five lakes of the same dataset and concluded, that unusually cold and nutrient-rich lakes will probably have algal blooms if their ice-free vegetation period increases. Besides effects on the lake ecology of algal blooms, ecosystem services such as aesthetic value, fishing or recreational activities would also be affected. In addition, Livingstone & Lotter (1998) state in their work on comparable lakes in Switzerland that the increased energy input due to climate change will lead to higher epilimnion temperature and to changes in aquatic ecology. They also expect direct ecological effects especially in fish habitats and indirect effects in oxygen concentrations and the characteristics of the thermal layers and mixing patterns of the lakes.

Based on the findings by Thompson et al., the underlying hypothesis is the following: It is suspected that the energy content of the incoming water, i.e. the temperature (energy input) of precipitation and runoff, makes up a significant proportion of the lake temperature. In order to identify the causes of the anomalies in the summer water temperature of the lakes, attempts are made to apply the most straightforward approaches possible. After an introduction to the basics of the parts of limnology and the state of the art for the analysis of lake water temperature that are important for this work, the approaches are presented at the end of the introduction and explained in detail in chapter 3.

## **1.1 Limnologic aspects**

As stated by Maniak (2016), the limnological conditions of standing water bodies are mainly determined by landuse and size of the catchment area, its morphological conditions, discharge regime, energy balance, currents and nutrient balance. Some fundamental information about different ways of classification for lakes, their physical processes and major influencing factors in terms of water temperature are given in this chapter. Although biological and chemical processes are an important part of limnology and to some minor extent correlated to the lakes physical properties, they are not part of this study and will therefore not be considered.

Already from the encyclopaedic definition of a lake as "any relatively large body of slowly moving or standing water that occupies an inland basin of appreciable size" (Lane, 2019), it becomes clear that especially the size of a water body can vary considerably. Also for the lakes investigated in this study, clear differences in the morphology can be observed. As Table 2.1 on 16 shows, the area of Kaltenbachsee is only 0.6 ha, while the largest lake Unterer Giglachsee measures 16.2 ha. Large differences can also be observed in terms of lake depth. For example, Unterer Landwiersee measures at its deepest point only 5.7 meters, while lake Weissensee measures 43.6 meters of water depth.

## Classification

Following the most comprehensive classification of lakes with regard to their formation after Hutchinson (1975), all of the lakes in this case can be identified as basins formed by glaciation. Most of them can further be described as so-called cirque lakes. These, mostly small and shallow ( $< 50$  m) lakes, are mainly located at the head of a valley. There, as a result of glacial excavation and scouring associated with the freezing and thawing of névé<sup>2</sup>, a concave shape has formed in the mountains surface. These bowl-shaped valleys usually are characterized by relatively steep valley walls and occur in practically every mountain range which has once been glaciated. If several lakes are arranged in an elongated valley one after the other at different heights, they are also called "paternoster" lakes. In the lakes studied, this "paternoster" form is for instant evident at Oberer, Mittlerer and Unterer Landschitzsee (see Figure 3.2 on page 23).

Some of the lakes in the area, which do not show the typical characteristics of cirque lakes, are of a different glacial origin. Both moraine and kettle lake forms would be possible, but the exact determination requires a more detailed investigation on site. One speaks of a moraine lake when a lake forms in the basin behind a terminal moraine, i.e. the accumulated glacial deposit that the glacier pushed out in front of it. Whereas a kettle lake is formed in deposited moraine material by the melting of large ice pieces which are detached from the main glacier tongue. (Lane, 2019; O'Sullivan et al., 2004; Wetzel, 2001)

In addition to their type of origin, lakes can as well be classified according to their thermal stratification and mixing characteristics during the year, which underlying processes are briefly explained in the next chapter. The most important basic research in this field has been done by Hutchinson (1975), who divided lakes into six groups according to their thermal characteristics:

- *amictic*: always ice-covered
- *cold monomictic*: ice-covered most of the year with occasionally thawing, but water temperature  $> 277$  K
- *dimictic*: one part of the year ice-covered and the other stably stratified; mixing in spring and fall
- *warm monomictic*: no ice-covered period; mixing once per year while stratified for rest of the year
- *oligomictic*: no ice-covered period; most of the time stratified with mixing at irregular intervals ( $> 1$  year)
- *polymictic*: no ice-covered period; stratified with several mixing periods per year

Lakes in which stratification is not possible, i.e. which are too shallow, are excluded from this classification. Building on this broadly accepted basic classification, some

---

<sup>2</sup>partially compacted granular snow

revised classifications followed, because newly obtained water temperature data from lakes showed, that the groups mentioned above were too imprecise.

Of the more refined classifications, the one from Lewis Jr. (1983) has been widely adopted, which mainly was set up to allow for a better classification of high-altitude lakes in the tropics. Concerning the lakes in this study, for example, the classification *polymictic* was divided into two subgroups:

- *discontinuous warm polymictic*: no ice-covered period; stratified for days or weeks with several mixing periods per year
- *continuous warm polymictic*: no ice-covered period; stratified at most for a few hours at a time

If one takes this reviewed classification by Lewis as a basis for the lakes of this work, most of the lakes fall into the category *dimictic*, which would agree with statements in the literature, which classifies the region of the *dimictic* lakes in Europe between 500 - 1,000 and 2,100 - 2,900 m a.s.l.. (Hutchinson, 1975) Whereas for the shallow lakes (e.g. Unterer Landwiersee, Moaralmsee, Angersee) also *discontinuous warm polymictic* could in some cases apply. For a precise classification of these lakes, further water temperature measurements at different depths would be necessary to obtain temperature profiles to properly identify mixing periods.

## Lake water temperature

As already mentioned in the previous section, the thermal stratification of lakes plays an important role in limnology, the underlying processes are summarized in the following.

In contrast to flowing waters, where the water temperature is approximately constant across the flow cross-section, the water temperature in lakes changes with depth due to differences in water density and the effects of atmospheric forces. (Maniak, 2016)

At about 277.15 K, water has its highest density of  $\rho = 1 \text{ g/cm}^3$ , which means that water with this temperature is at the deepest point of the watercolumn and is superimposed by warmer or colder water. Due to this density anomaly of water, seasonal thermal stratification of varying stability occurs in sufficiently deep lakes.

If we look at the lakes in this study, they are covered by ice during the winter months. Since the density of ice at 273.15 K is  $0.9168 \text{ g/cm}^3$ , while that of water at the same temperature is  $0.9999 \text{ g/cm}^3$ , the ice floats on the water surface. Therefore, an inverse thermal stratification is observed, i.e. the water temperature at the bottom of the lake is around 277.15 K (due to the high density) and decreases towards the water surface. The overlaying ice cover furthermore acts as an isolating layer and protects against turbulence and therefore stabilizes the inverse stratification.

As the ice thaws in spring, a more or less even uniform distribution of temperature and thus also density in the water column develops. Wind-induced currents at the water surface now trigger an exchange within the water column and thereby transport heat to the deeper layers of the lake. In the course of spring, the surface layer of

the water warms up gradually faster, which leads to a lower density and thus makes it more difficult for external influences to mix the water column. The upper, relatively evenly warm and turbulent layer is called *epilimnion*, while the deeper, cold and relatively motionless part of the lake is called *hypolimnion*. The transition between the warm and cold layers, where the temperature drops rapidly with increasing depth, is called *metalimnion*. This stratification stability against energy input by wind and mixing is described by the gradient  $d\rho/dh$ , hence the change of density within a water column, which at 293.15 K is about  $0.23 \cdot 10^{-3} \text{ g}/(\text{cm}^3 \text{ K})$ , and some 20 times greater than at 273.15 K. Whereby, the higher the temperature differences between the upper and lower layers and the higher the water temperature, the greater the stability of stratification. (Hutchinson, 1975)

### Influencing factors

The factors influencing water temperature have been the subject of research for several centuries and still continue to provide the scientific community with questions today.

Various approaches to describe the influencing factors on water temperature of lakes can be found in literature. (Hutchinson, 1975; Edinger et al., 1968) Although the scientific community is in agreement about the forms of energy that act on and out lake, the structure of all formulas is similar, but they simplify the various components in different ways.

From a physical point of view, the net rate of the heat exchange processes  $H_{net}$  is calculated by Piccolroaz et al. (2013) with

$$H_{net} = H_s + H_a + H_w + H_e + H_c + H_p + H_i + H_d \quad (1.1)$$

whereby the different fluxes are schematically shown in Figure 1.1.

$H_s$  indicates the net heat flux from short-wave solar radiation and  $H_a$  the net long-wave atmospheric radiation, with the long-wave radiation emitted from the water is described by  $H_w$ .  $H_e$  denotes the rate of heat loss by evaporation and condensation (latent heat flux) and  $H_c$  the rate of heat conduction (sensible heat flux).  $H_p$  stands for the heat flux due to precipitation,  $H_i$  represents the heat input/output by inlets and outlets and  $H_d$  describes the heat flux exchanged with deeper water from the hypolimnion. The sum of incoming direct and diffuse solar radiation, also called global radiation, can be measured directly with a pyranometer, while the size of the reflected ratio within  $H_s$  depends on various factors, such as albedo  $r_s$ , cloudiness, latitude and shadowing due to local topography. The net long-wave radiation  $H_a$  of the atmosphere depends on the temperature and composition of molecules in the overlying atmosphere and can be described by the long-wave reflectivity of the water  $r_a$ , the Stefan-Boltzmann constant  $\sigma$ , the water temperature and the emissivity of the atmosphere. Rate of heat loss by conduction  $H_c$  and evaporation  $H_e$  depend in various ways on the water surface temperature, air temperature, water vapor pressure and wind conditions. (Edinger et

al., 1968; Piccolroaz et al., 2013)

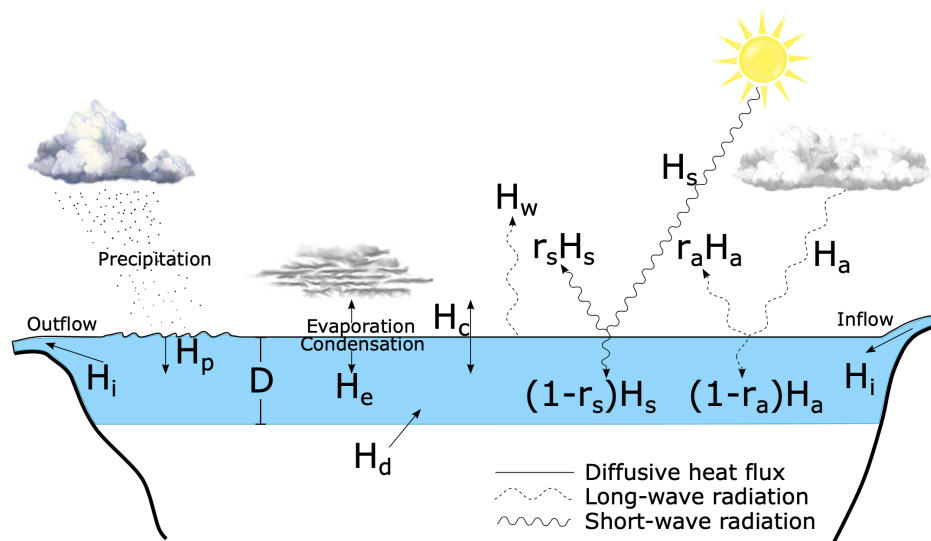


**Figure 1.1:** Main heat fluxes interacting with the water surface, taken from Piccolroaz et al. (2013)

Which of these processes has the greatest impact on water temperature varies from lake to lake, and studies frequently come to different conclusions about which processes are negligible and which are significant. According to Sharma et al. (2008) the water temperature of lakes is basically influenced by the local climate, the lake morphology, the water chemistry and the surrounding topography. Furthermore, Hutchinson (1975) states that also the altitude at which the lake is located determines the temperature regime, as an increase in altitude is very roughly equivalent to an increase in latitude. Marti & Imboden (1986) analyzed the influence of meteorological factors on the water temperature of the Swiss Semperssee on the basis of the net rate of heat exchange processes, but concluded that other factors such as the contribution of inflows and outflows only play a negligible role. In this context it must be noted that the Semperssee with an area of 14.1 km<sup>2</sup> is almost 90 times larger than the largest lake of this study (Lower Giggachsee with 16.2 ha). For smaller lakes, inflows and outflows could therefore have an impact on water temperature and should be considered, as the study by Strøm from 1935 cited in Hutchinson (1975) on page 446 which indicates, that meltwater has an influence especially on lakes with smaller drainage basins.

## 1.2 Modelling types

While hydrological modelling in general is a common practise in hydrology, i.e. creating rainfall runoff models for flood protection measures or hydropower operating, temperature modelling of lakes and streams is getting more attention, as the impacts of climate change are already noticeable and need further research.

To explain and predict the water temperature of lakes using external factors, two main types are used: physically-based and statistical models. In the following sections,

the most common model types will be characterised and their implementation will be described by means of corresponding studies.

## Physical oriented approaches

Physically-based models are developed on processes for which descriptive equations are available that can be well reproduced in defined, spatially homogeneous stationary test environments. These processes are then applied more or less directly to the real world, i.e. a three-dimensional, spatially heterogeneous and time-changing environment.

Edinger et al. (1968), for example, have analyzed the influence of meteorological factors on water temperature, focusing on the underlying physical principles of heat exchange processes.

Using the equilibrium temperature  $T_e$  and the thermal exchange coefficient  $K$  they defined methods to estimate the water temperature  $T_s$  and net rate of heat exchange  $H_{net}$ .

$$H_{net} = K(T_e - T_s) \quad (1.2)$$

As shown in Equation 1.2, the net rate of heat exchange across the water surface is therefore a function of the difference between the actual water temperature at the surface  $T_s$  and an equilibrium temperature which is reached when  $H_n$  is 0.  $K$  describes the rate at which the water temperature reacts to the heat exchange processes. These exchange processes, such as short- and long-wave radiation, conduction and evaporation, occur mainly at the air-water interface and are measurable in the field.

When the formula is applied, a delay between maximum water temperature and maximum equilibrium temperature can be observed, which represents the heat capacity of the water and its reaction to meteorological factors. The range of the reaction time varies on a seasonal average between a few days, whereas it amounts to a maximum of 6 hours on a daily basis. While in the ideal case the maximum equilibrium temperature occurs during midday, the maximum water temperature occurs on average between afternoon and evening. This time lag is influenced to a large extent by the depth of the water; the greater the depth, the greater the time lag.

Building on a general heat balance equation (similar to Equation 1.1) and the equilibrium water temperature of Equation 1.2, Livingstone & Imboden (1989) investigated the annual variation of Lake Aegeri in Switzerland based on 12 years of monthly mean meteorological and surface temperature data. They discovered that with comprehensive meteorological data on air temperature, air pressure, wind speed, humidity, cloud cover and global radiation it is possible to calculate the heat budget using the heat balance equation. Thereby, the two processes of absorption and emission of long-wave radiation are the main factors in the determination of the heat balance. In terms of calculating the equilibrium temperature Livingstone & Imboden found that cloudiness and humidity

have a greater influence than wind and air temperature.

Also worth mentioning are Marti & Imboden (1986), who have carried out a high-resolution, physics-based investigation of Sempachersee in the Swiss midlands. For this, extensive measurement data were used, including water temperature at different depths as well as all relevant meteorological factors at different altitudes, such as wind speed, air temperature, solar radiation, humidity, wind direction and buoy orientation, all of which were measured from a buoy in the middle of the lake. A similar equation as Equation 1.1 was used for the theoretical calculation of thermal energy flows, but heat fluxes due to precipitation, inlets and outlets and by exchange with deeper water were neglected due to their small contribution. In their study, the measured water temperature could be well simulated by the heat flow calculated from meteorological data which validated the concepts for calculating the heat exchange between water and atmosphere. However, they recommend further investigations for the direct measurement of long-wave atmospheric radiation, as this results in large fluctuations in the annual balance. Furthermore, they note that vertically measured temperature profiles in lakes are only a snapshot of the momentary state, i.e. the temperature changes in space and time. Especially the wind plays a bigger role than initially assumed, as it is responsible for a vertical mixing of the water column, which in turn has a great influence on the heat flow from the lake into the atmosphere.

## Statistical approaches

Besides physical oriented approaches, there are also statistical approaches, which are used to estimate the measured water temperature with one or more measured external factors. Especially studies where linear and multiple linear regression are chosen as modelling approach can be found in the literature. (McCombie, 1959; Sharma et al., 2008; Matuszek & Shuter, 1996)

A regression analysis aims to establish a linear relationship by

$$f(y) = a + bx \tag{1.3}$$

between an observation  $y$  and an explanatory  $x$  variable. In multiple linear regression several explanatory variables are used. The key figures of the regression line are  $a$ , which represents the intersection with the  $y$ -axis, and  $b$ , which indicates the mean change of  $y$  for a change in  $x$  and thereby describes the slope of the line. (Hedderich & Sachs, 2018; Messer & Schneider, 2019)

Due to increased computing power, machine-learning approaches such as artificial neural networks are more and more widely applied to establish a relationship between predictor and response variables. They imitate the learning process of the mammalian brain, whereby the weighing of predictor variables (input neurons) is controlled by one or more hidden layers and passed on to the response variable (output neuron). To set

the weights within the hidden layers, neural networks must first be configured using a training dataset. (Sharma et al., 2008)

As one of the first studies, McCombie (1959) conducted a comparison of monthly means of air and surface water temperature at three Canadian lakes and fitted a linear regression model for each month to the data. They thereby found a close correlation between monthly means of air and surface water temperature which allowed to identify two different phases: during May, June and July the variation of water and air temperature from year to year is fairly similar and in September, October and November averaging over several years resulted in more stable water than air temperature. The authors of the study associated these results with the greater heat storage capacity of water compared to air. They conclude that the most reliable way to deduce water temperature from air temperature is to have a sufficient database for an accurate calculation of the monthly regression coefficients.

Matuszek & Shuter (1996) used daily air and water temperature from 14 lakes in Ontario to create lake-specific empirical models for predicting water temperature during the ice-free period using multiple linear regression. For this purpose, the mean air temperature and the day of the year were chosen as main predicting parameters. Matuszek et al. found that water temperature did not correspond to air temperature in a constant manner: although water temperature followed air temperature relatively closely in spring, water temperature was significantly higher than air temperature in summer and autumn, which is in line with the findings by McCombie (1959). They also decided to, like Edinger et al. (1968), introduce a lag-time, which causes the water temperature to lag behind the air temperature. This means that the air temperature is averaged over a number of previous intervals and related to the current water temperature, whereby a range of 5 to 20 days was finally found to deliver optimal results. With the creation of annual models for the lake with the longest available measuring period of 22 years they achieved root-mean-square deviation (RMSE hereafter) values of 0.76 to 1.24 K. For the model variant for which they used all 22 years of the data set for the parameter calculation, they obtained RMSE values of 0.87 to 2.10 K. Another model variant, where they additionally took into account short-term and long-term air temperature averages, did not significantly improve the RMSE compared to the previous model variant. However, there were atypical years with extreme climatic conditions in which the regression coefficients differed significantly and the water temperature could not be determined based on the air temperature and the day of the year. Looking ahead, the authors suggest that it might be easier to create multiyear models for lakes that do not freeze annually.

In a paleolimnology focused study by Livingstone & Lotter (1998) 17 lakes of the Swiss Plateau were investigated, whether and in which way their summer water temperature can be related to the regional air temperature. For the air temperature, values of 15 different measuring stations were averaged, related by means of a lapse rate to a reference height of 500 m a.s.l. and assumed as uniform for an area of 20,000 km<sup>2</sup>. In

a further step also the measured water temperature was corrected with the same lapse rate (due to the assumed correlation of the two) to a reference altitude of 500 m a.s.l.. When comparing the air and water temperature graphs, it was noticed that especially in the winter half of the year (October - March) the water temperature at the lake surface does not show any significant short-term agreement with the air temperature. This can be explained by the fact that the mixing condition of the lakes has a dampening effect on the water temperature. Like in the previous studies, the correlation between water and air temperature was significantly higher in the summer months (June, July, August) with its highest value in July ( $r^2 = 0.84$ ). And once again, the authors introduced a lag-time, i.e. a temporal delay between air and water temperature to improve results. In addition, the authors note that especially the water temperature at the lake surface clearly corresponds to the air temperature, the correlation decreases rapidly with water temperature measured at greater depths. In general, increases of air temperature are better represented by the the water surface than equivalent temperature decreases, which can be explained by the raised thermal stability of the epilimnion with increasing water temperature and the dampening effect of mixing conditions with decreasing water temperature. Finally, the authors warn that the dependence between air and water temperature could additionally be affected by topographic shading and altitude-dependent changes in radiation.

Another study by Livingstone et al. (1999) investigated the decrease in summer lake surface water temperature of 10 Swiss alpine lakes with increasing altitude and compared it with the regional air temperature to develop a clearer understanding of their relationship. As all previous studies, they too found that although the lapse rate of water temperature in the summer months of June, July and August is greater than that of air temperature, the two are nevertheless very similar. While the measured water temperature during these months is higher than that of the air, the temperature difference increases with altitude. In one of the lakes, significantly lower surface water temperature was measured than the linear extrapolation of the regression lines would suggest. According to Livingstone et al. this is related to the local topography, since the shading by a nearby high cliff reduced the amount of received solar radiation. In general, they conclude that the linear relationship between air and water temperature lapse rates only applies to lakes up to about 2,000 m a.s.l., while lakes above this altitude tend to form an ice-free water surface only for a short time in summer and are therefore decoupled from atmospheric forcing. Furthermore, they note that daily variations in water temperature do not represent the mean value and therefore recommend using lower temporal resolutions for analysis. In addition, water temperature can be influenced by other factors such as shading, partial ice cover and melt water inflows, which can disturb the simple linear relationship between air and water temperature.

Kettle et al. (2004) try to estimate the mean daily lake surface water temperature of 15 lakes in southwest Greenland with the input parameters air temperature, theoretical

clear-sky solar radiation and lake morphology and an empirical approach. In order to show the slower response of water temperature to changes in air temperature, an exponential smoothing filter to air temperature is applied instead of a lag-time, resulting in a 35 % decrease in error compared to no filter when modelling the water temperature. The parameters necessary to create the regression model depend to a large extent on the thickness of the epilimnion and thus on the thermal stratification at each time step. Since this mixing depth is not easily measurable, a relationship between maximum lake depth, lake surface area and salinity was established. Furthermore, they found that the lakes were affected by wind to varying degrees, which is also difficult to measure due to its heterogeneous spatial distribution and is identified as the main source of error in this region. Due to the comparatively small data base of three years, Kettle et al. emphasize that it would be unwise to apply their calculated model parameters to other lakes and times outside the model-building period.

In a study by (Sharma et al., 2008) data about 2,348 lakes in Canada was used to compare different modelling approaches for predicting maximum lake water temperature at a large scale. The four used statistical models are multiple regression, regression tree, artificial neural networks and Bayesian multiple regression. Each model was tested with four to 17 predictor variables and afterwards the performance of the different approaches was compared. It was found that mean air temperature in July explains the greatest variation in maximum surface water temperature, while mean annual air temperature and the day of the year are also important input variables. Both multiple regression models and artificial neural networks show similar predictive capabilities, but when compared to the effort required to build the other models, multiple regression is recommended by the authors as a good method for similar datasets. However, a careful preparation of data should take place beforehand, since multi-collinearity and error distribution can worsen the output. In contrast to previous studies lake morphology and water chemistry explained little variation in temperature, which could be due to the fact that these studies were spatially concentrated in smaller areas and that this study was on a large scale.

### **1.3 Aim of the thesis**

This thesis is intended to form the basis for an initial assessment of the lakes hydrological conditions and attempts to identify the causes of the anomalies in the lakes' summer water temperature by using approaches that are as straightforward as possible. Based on Thompson et al. (2005) findings, the underlying hypothesis is the following: It is suspected that the energy content of the incoming water, i.e. the temperature (energy input) of precipitation and runoff, makes up a significant proportion of the lake temperature.

As described earlier, the study by Thompson et al. (2005) leads to the question how the different summer water temperatures of the lakes can be explained. Since physically based models require extensive meteorological data such as dew point temperature,

wind speed, solar radiation and total cloud cover, they are out of consideration for this thesis. The available SPARTACUS data on daily air temperature will be related to the individual catchment areas by means of linear regression (see 3.3 for details) and afterwards compared with the respective water temperature to search for similarities. Since, as has been demonstrated in other studies, similar physical processes influence the air and surface water temperature. (McCombie, 1959; Matuszek & Shuter, 1996; Livingstone & Lotter, 1998) As our available dataset shows that maximum air and water temperatures are measured on average in the month of August, a correlation between air and water temperatures during the summer months of June, July and August is considered, with thermal stability suppressing the mixing processes. (Livingstone & Lotter, 1998) Otherwise the water temperature of earlier months could still be strongly influenced by melting of the ice cover or snow melt in the catchment area, which would reduce the correlation between air and water temperature.

To support the initial hypothesis, three approaches were chosen, which increase in their complexity and are briefly introduced in the following.

The first approach is limited to the terrain model and the associated lapse rate of the air temperature, which implies a decrease in temperature with altitude. Founded on the assumption that the lakes' water temperature is largely influenced by diffuse inflow from its respective watershed, the topography of the watershed itself can be used to derive information on the thermal character of the lake. (cf. Livingstone 2005 qtd. in Šporka et al. (2006) on page 82) In other words, for lakes with a low water temperature, a comparatively high proportion of their catchment area should lie in high altitude regions. Lakes with relatively high water temperature should show a bigger tendency to have a higher share of their catchment area at lower altitudes. For this purpose, the lakes are divided into five groups according to their mean summer water temperature and elevation at lake level. By creating elevation distribution plots, the catchments of each group can be graphically compared.

For the second approach, the terrain model is supplemented with spatially interpolated data on air temperature. By combining local lapse rates for air temperature with the topography of the catchment area, it should be possible to make general statements about their air temperature characteristics during summer into the individual lakes. In a further steps these air temperature characteristics will then be compared with the water temperature of the respective lakes to check for potential connections. (McCombie, 1959; Matuszek & Shuter, 1996; Livingstone & Lotter, 1998)

The third approach aims to include a simplified energy input into the catchments by supplementing topography and air temperature information with spatially interpolated data on precipitation. Furthermore, this approach does not only refer to the summer months, but to the whole year, which also allows an estimation of the snow input.

What distinguishes these approaches from the earlier study conducted by Thompson

et al. is first of all the different source of air temperature data. While they made use of 13 local meteorological stations in a radius of 75 km and six regional stations to generate daily values for the entire time span of the water temperature measurements, I applied temperature and precipitation grid data from ZAMG. It is assumed that this spatially interpolated data with a resolution of 1 x 1 km will lead to a more precise representation of reality with regard to the hydrological conditions within the catchment areas by providing a more detailed air temperature and precipitation lapse rate dimensioning. Furthermore, the current study features a more detailed spatial mapping of the catchment areas through the used digital elevation model. Thompson et al. (2005) based their study on previous GIS processing by Kum (1999), created within the EU project CHILL-10,000<sup>3</sup>. Here, morphological information of the lakes as well as data on the catchment areas, such as land cover and slope orientation, was included. The digital terrain model that was used in their GIS study was created using a photogrammetric analysis of false-color images with an average scale of 1:15,000. The accuracy of the resulting model varies between 1 - 20 m, depending on the shape of the terrain. For this work, however, I used airborne laserscan data with a spatial resolution of 1 m in order to create the terrain model. The accuracy of this method is about 15 cm, which contributes to a more precise representation of the relatively small catchment areas.

This thesis is divided into five sections. Firstly, the following chapter provides a data description, followed by an illustration of the different processing and the used methods in chapter three. Afterwards, the results are presented in chapter four prior to a discussion and possible perspectives for further analysis in chapter five.

---

<sup>3</sup>Climate History as recorded by ecologically sensitive arctic and alpine Lakes in Europe during the Last 10,000 years: a multiproxy approach

## 2. Data description

This chapter provides general information about the study area and gives an overview of the data used in the course of this study.

### 2.1 Study area

The 44 investigated lakes are situated in the Eastern Alps, more precisely in the Niedere Tauern Alps, roughly 80 km to the south-west of Salzburg (see Figure 2.1). 13 of them are located in the federal state of Styria and the remaining 31 in the federal state of Salzburg.

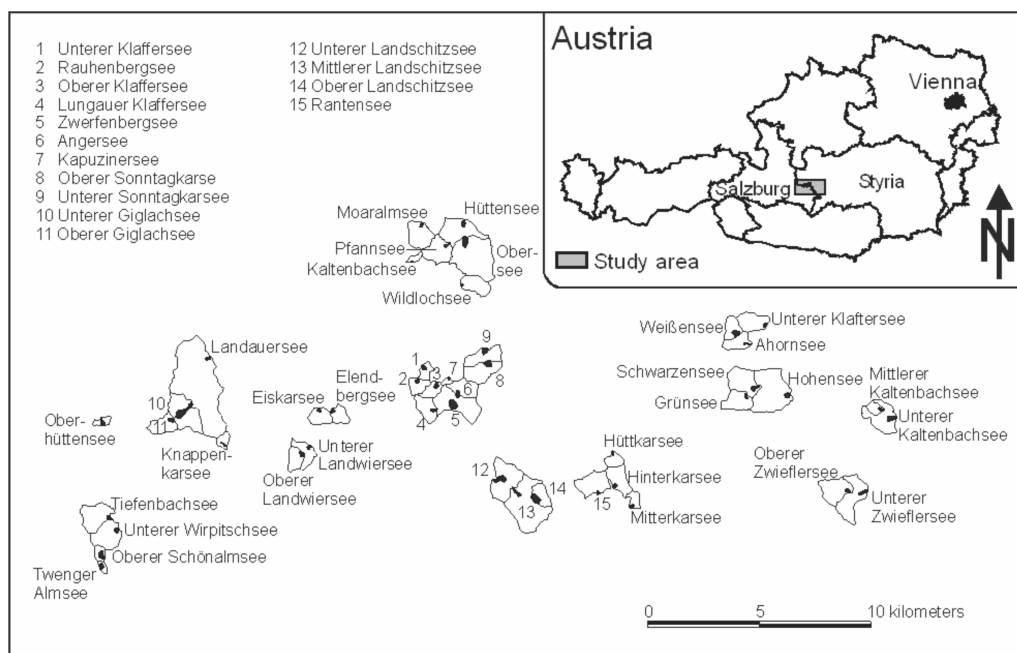


**Figure 2.1:** Location of the study area and the lakes, taken from Thompson et al. (2005)

The study area itself extends about 25 km from north to south and 40 km from east to west with an elevation ranging from 723 m a.s.l. in the valleys to 2,861 m a.s.l. at its highest peak. Table 2.1 shows some information about the coordinates of the lakes, their height in metres above sea level (m a.s.l. hereafter) and the two morphological parameters concerning lake depth and surface area. The lakes themselves are located within an altitudinal range of 807 m, with Hüttensee as the deepest at 1,503 m a.s.l. to Oberer Klaffersee as the highest at 2,310 m a.s.l. (median: 1,980 m a.s.l.). The median value of all the lakes investigated is 3.3 ha, with only three having a water surface larger than 10 ha and another eight featuring a water surface larger than 5 ha. The 33 remaining lakes have a water surface of less than 5 ha, the smallest lakes being Hüttkarsee with 0.9 ha and Kaltenbachsee with 0.6 ha. With regard to their maximum water depth, a greater degree of variability can be observed. For instance, the Unterer Landwiersee with its 5.7 m water depth is the shallowest of the lakes, while

the Weissensee is the deepest with 43.6 m (median: 13.5 m). Furthermore, it can be stated that the water surface is by no means an indicator of lake depth. The Unterer Klaffersee, for example, with its relatively small surface area of 3.7 ha, measures 39.6 m in depth, while the Unterer Landschitzsee (11.3 ha), which is three times as large, is comparatively shallow with 15.8 m.

Id	Name	Easting Y (m)	Northing X (m)	Elevation (m a.s.l.)	Max. depth (m)	Area (ha)
1	Ahornsee	499474.9	241231.1	2068.5	6.9	2.5
2	Angersee	486296.5	238968.5	2096.4	6.3	3.1
3	Eiskarsee	480128.0	238409.0	1941.5	14.2	2.7
4	Elendbergsee	480697.0	238432.0	2217.9	21.0	3.3
5	Gruensee	499270.5	239089.5	1984.0	6.7	3.0
6	Hinterkarsee	493323.8	234900.8	2073.4	11.3	1.8
7	Hohensee	501307.0	239048.0	1540.7	7.3	4.6
8	Huettensee	486635.0	246933.0	1502.6	7.7	4.7
9	Huettkarsee	493322.0	236435.0	2137.4	7.8	0.9
10	Kaltenbachsee	484298.0	244978.0	2215.0	9.9	0.6
11	Kapuzinersee	486019.0	239872.0	2146.3	20.0	2.2
12	Knappenkarsee	475931.0	236690.0	2258.7	8.0	1.8
13	Landauersee	475224.0	240753.0	1652.5	16.6	3.6
14	Lungauer Klaffersee	485455.0	238431.0	2198.1	17.7	4.4
15	Mitterkarsee	494093.0	233879.0	2149.3	11.5	2.7
16	Mittlerer Kaltenbachsee	505464.0	238326.0	1911.4	9.5	2.3
17	Mittlerer Landschitzsee	488779.0	234878.0	1939.1	20.3	6.0
18	Moaralmsee	484722.0	246758.0	1824.8	5.9	2.0
19	Oberer Giglachsee	473573.0	237945.0	1930.1	10.5	3.4
20	Oberer Klaffersee	485402.0	239626.0	2310.0	32.5	5.1
21	Oberer Landschitzsee	489741.0	234219.0	2066.5	13.6	8.7
22	Oberer Landwiersee	479424.5	236394.0	2046.4	13.4	4.0
23	Oberer Schoenalmsee	470482.0	231661.0	2111.9	21.6	5.1
24	Oberer Sonntagkarsee	487769.0	240532.0	2062.4	17.5	6.5
25	Oberer Zwieflersee	503865.0	234590.0	1925.4	18.6	3.0
26	Obersee	486595.0	246093.0	1672.6	23.4	7.0
27	Pfannsee	485964.5	245865.5	1968.2	7.7	1.5
28	Rantensee	492586.0	234523.0	1879.8	7.6	2.2
29	Rauhenbergsee	484585.0	239777.0	2263.7	26.3	2.7
30	Schwarzensee	499863.0	239366.0	1916.0	13.3	3.7
31	Tiefenbachsee	470835.0	233374.0	1844.2	8.0	3.3
32	Twenger Almsee	470243.5	231287.5	2118.6	33.3	2.9
33	Unterer Giglachsee	474383.0	238683.0	1922.0	18.0	16.2
34	Unterer Kaltenbachsee	506013.5	237987.0	1749.0	32.0	5.6
35	Unterer Klaffersee	484696.0	240305.0	2103.3	39.6	3.7
36	Unterer Klaftersee	500195.9	242235.0	1884.2	11.4	1.6
37	Unterer Landschitzsee	487898.0	235135.0	1783.5	15.8	11.3
38	Unterer Landwiersee	479728.0	236746.0	1977.1	5.7	1.5
39	Unterer Sonntagkarsee	487462.0	241137.0	1960.6	25.9	4.8

Id	Name	Easting Y (m)	Northing X (m)	Elevation (m a.s.l.)	Max. depth (m)	Area (ha)
40	Unterer Wirpitschsee	471121.7	232955.7	1701.0	8.0	2.7
41	Unterer Zwieflesee	504676.0	234729.0	1809.5	19.4	4.2
42	Weissensee	498937.1	241672.9	2227.1	43.6	6.3
43	Wildlochsee	486462.0	243923.0	2108.5	6.4	1.3
44	Zwerfenbergsee	486128.5	238353.5	2026.3	36.5	10.8

**Table 2.1:** General information about the lakes: as coordinates (after MGI / Austria GK M31), elevation, maximum depth, water surface.

## Predominant catchments

The federal border is almost congruent with the division of the two prevalent predominant drainage basins. As Figure 2.2 shows, all of the lakes located in Styria drain into the Enns and all of the lakes on the Styrian side drain subsequently into the Mur river.

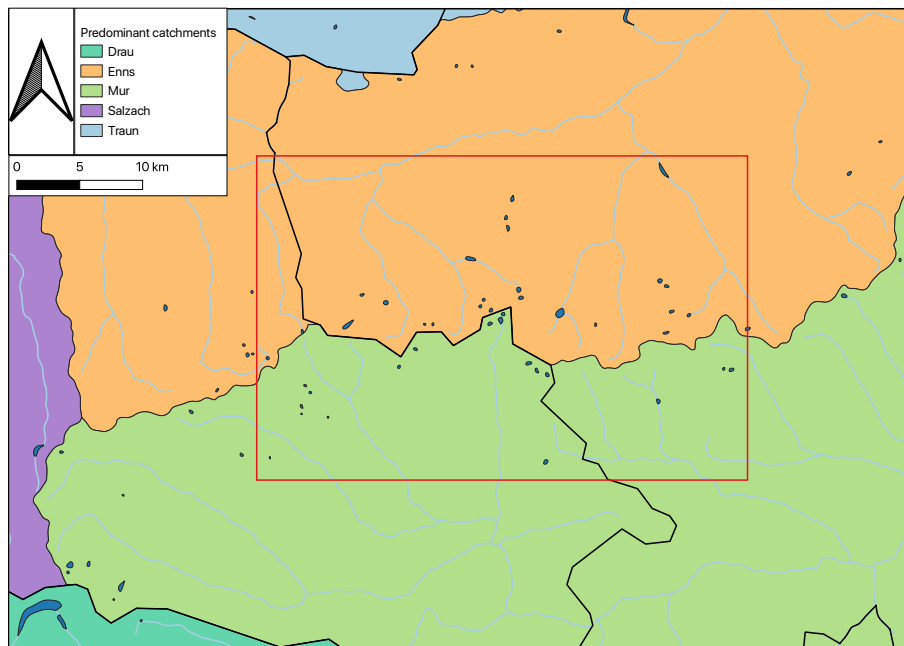


**Figure 2.2:** Predominant catchments of the research area (red box) as of .

## Land cover

Data collected from the European CORINE<sup>1</sup> Land Cover (CLC) project depict that most of the higher elevated areas of the study area are only sparsely covered with vegetation, and in some spots, bare rock is even prevalent (cf. Figure 2.3). With decreasing height, the land cover changes into natural grassland and transitions into coniferous forest with the treeline between 1,700 and 1,800 m a.s.l.. In line with the Timm's claim (ctd. in O'Sullivan et al. (2005)), that high alpine lakes are usually located above the tree line, one hardly notices any trees in the catchment areas of the lakes. Table A.2 in

<sup>1</sup>Coordination of Information on the Environment

Appendix A shows the percentage and areal distribution of each land cover class within the catchment areas.

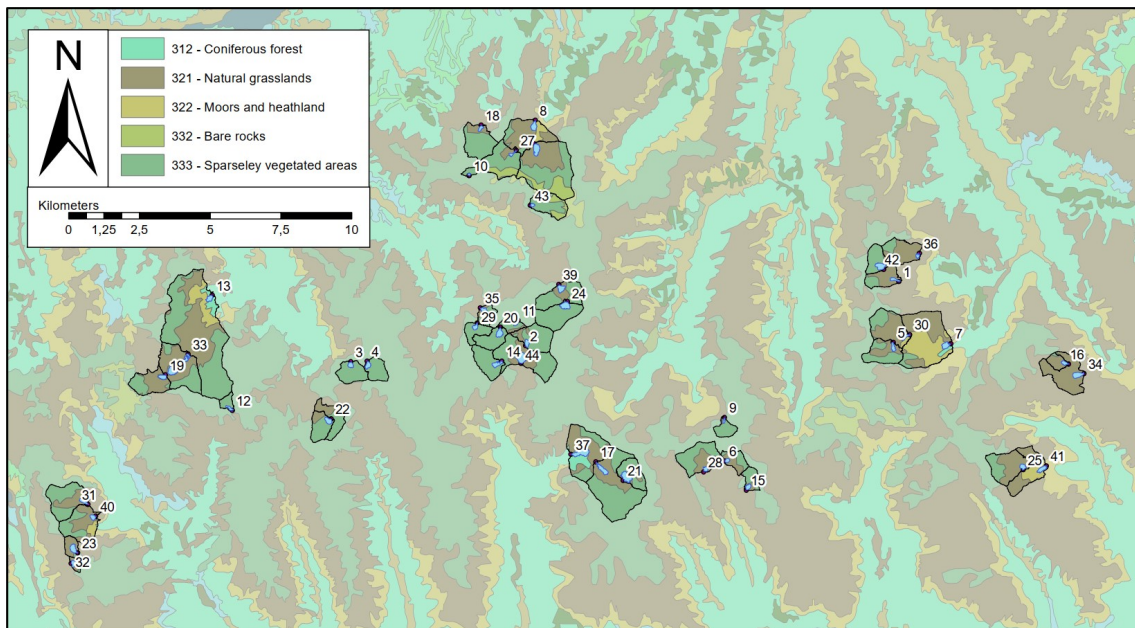


**Figure 2.3:** Land cover according to CLC (as of 2018).

## Geology

Figure 2.4 shows the geology of the study area according to the Geological Survey of Austria (2005). On a wider scale, the area under investigation is located at the border between the East Alpine Permomesozoic and the East Alpine Crystalline. It can be seen that most of the catchments are located on metamorphic bedrock of the East Alpine Crystalline, consisting mainly of granite, gneiss and slate. In the western parts of the research area, phyllite is predominant in some areas. Although the Lower Tauern region has with the Northern Limestone Alps a karst system to its northern bounds, no carbonate bedrock can be found within the lakes' catchments. Since they have no shares in catchment areas, it can be assumed that the hydrological processes of these lakes are not influenced by any karst water. With the lakes being underlain by crystalline rocks whose permeability is low, the sources of incoming water can be limited to precipitation falling on the lake surface, surface water inflows, and groundwater seeping into the lake. Since the inflowing groundwater has a comparatively small contribution compared to the other two sources, it will not be given special consideration.

## 2.2 Lake water temperature

First of all, the used temperature data of the 44 lakes was taken from a study by Thompson et al. (2005), who took measurements of the epilimnion water temperatures with a temporal resolution of two- and four-hourly intervals from July 1998 to September 2003. The researchers further measured the water temperature of another lake, the Oberhüttensee, which compromises a total of 45 lakes. Since this lake is the only one

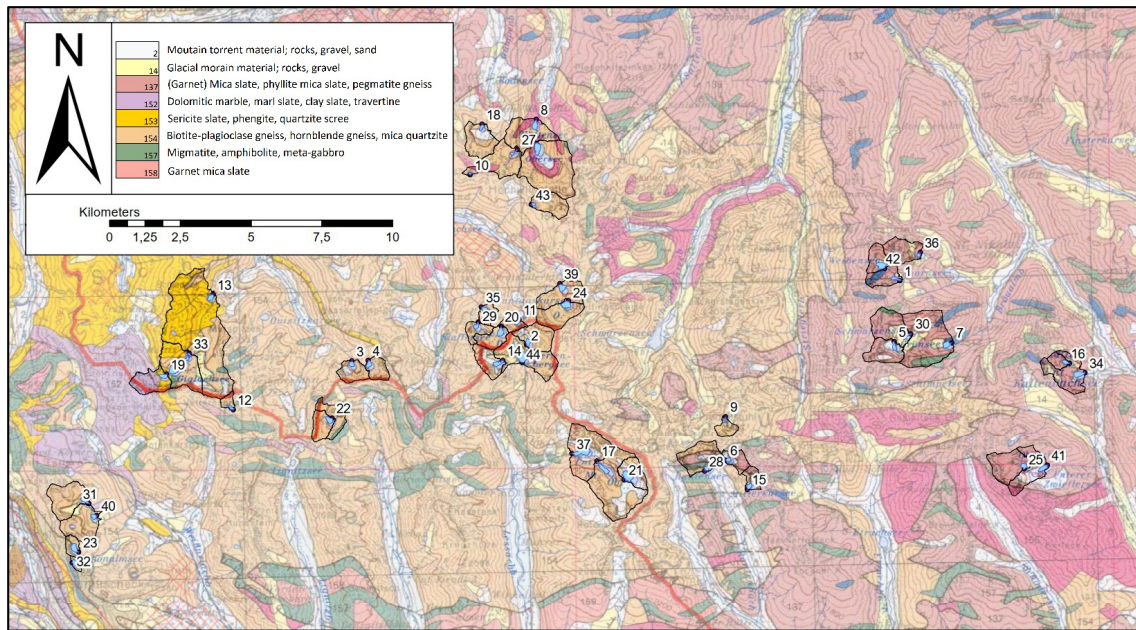


**Figure 2.4:** Geology of the study area (as of Geological Survey of Austria (2005)).

that does not belong to a group of adjacent catchment areas, it is excluded from this study.

As far as the measuring instruments are concerned, thermistors (8-bit MINILOG-TR, manufactured by Vemco Ltd., Shad Bay, Nova Scotia, Canada) with a resolution of 0.1 K from -4 to 20 K and an accuracy of 0.2 K (Geo Scientific Inc., 2001) were employed. Two thermistors were installed at each lake as low as 1.4 to 3.3 m, which resulted in an almost continuous record for most of the lakes. Though there are some minor gaps in the measured data, at least one of the thermistors consistently functioned in most cases. Some thermistor data are, however, missing from Lungauer Klaffersee, Oberer Landwiersee and Weissensee, which limits the examinations in these cases to approximately one year. Arguably, these losses of data might have originated in the landing of the measuring instruments or the lack of the recovery of the measuring instruments due to turbid water conditions or the plain lake extent (cf. Thompson et al. (2005)). In addition to that, for Unterer Giglachsee and Wildlochsee, even though the data sets are not complete, more data points are available than for the previous three lakes. With regard to these two lakes, no additional information is provided in the paper. Since the authors of the study have since retired or are no longer contactable, I could not determine whether the data were subsequently lost or not collected at all. However, studies by Schmidt, Kamenik, Kaiblinger, & Hetzel (2004) and Schmidt, Kamenik, Lange-Bertalot, & Klee (2004) based on the same data show that the data are still suitable for reading ice-free periods, as well as ice-on and ice-out dates, and provide a solid basis for further analysis of the LSWT and its relationship to air temperature.

## 2.3 Elevation data

As part of open access data, a digital elevation model (DEM) with a resolution of 10 x 10 m is available via <https://www.data.gv.at/> in Austria. Since the analysed lakes are in some cases rather small-sized, it may be beneficial to aim at a dataset with a higher resolution. For that reason, I contacted the involved federal states of Styria and Salzburg and obtained DEMs from airborne laser scans with a resolution of 1 x 1 m. The elevation data for the study area were obtained by the federal state authorities of Styria and Salzburg in form of LIDAR data with a spatial resolution of 1 m and delivered in form of a DEM, therefore obstacles like vegetation or buildings were already removed from the dataset. Since the study area is located at the borderline between the two federal states, it was necessary to combine the two DEMs into one model by using a geographic information system. The high spatial resolution is required in order to define the relatively small catchment areas of the lakes as precisely as possible and further allows for the identification of minor tributaries.

## 2.4 Temperature and precipitation data

Due to the remote location of the lakes, there are few meteorological stations nearby that provide continuous data for the researched period, which is why the SPARTACUS<sup>2</sup> dataset was utilised.

This spatial climate dataset project is financed and operated by the Central Institute for Meteorology and Geodynamics (ZAMG) and covers Austria's national territory with about 61,000 raster fields.

It is based on a spatial interpolation method, which was originally developed for Switzerland by C. Frei and focuses on mountainous regions with complex topography. In order to adapt the interpolation method to the geography and the measuring station network of Austria some changes were made. For example, 150 stations are used for air temperature in Austria and an additional 38 stations in neighbouring countries in order to improve the simulation of the border areas. Some measuring stations have been chosen to cover local features such as cold-pools, summits or city centres. The spatial interpolation method is based on the superposition of large scale background temperature fields with regional residual fields. Background fields refer to large scale horizontal changes of air temperature and topography related vertical temperature profiles. Residual fields cover regional variations, such as cold-pools within valleys. The so called non-euclidean distance metric is used to identify topographic barriers and their influence on air temperature.

For the collection of precipitation data 523 Austrian stations and 43 stations abroad are used. To calculate the daily precipitation sums, a distinction is again made between background and residual fields. Background fields consist in this case of by Kriging with external drift interpolated mean monthly precipitation values. The daily relative

---

<sup>2</sup>Spatiotemporal reanalysis dataset for climate in Austria

anomalies, which are determined by angular distance weighting, indicate the residual fields.

Each raster field measures 1 × 1 km and features the daily minimum (T<sub>n</sub>) and maximum (T<sub>x</sub>) air temperature in °C, as well as the daily precipitation sum in mm. To make a display of temperatures below 0 °C clearer, they are converted to K. The daily resolution for the precipitation data is thereby defined as the time span from 7 a.m. of the current day to 7 a.m. of the following day, the standard reading time in Austria. For air temperature, however, the daily T<sub>n</sub> and T<sub>x</sub> are defined as the extremes over the 24 hour span between 7 p.m. of the previous and 7 p.m. of the current day. The dataset extends back to 1961 and is constantly updated. It was developed for climate monitoring and modelling, as well as for the detection of potential climate change signals, but can also be used for modelling hydrological processes. (Hiebl & Frei, 2016, 2018)

# 3. Methods

This chapter deals with the applied methods consisting of the data preparations, the data processing, and the different work steps taken for each approach.

## 3.1 Data preparation

### Lake water temperature

The measured datasets of the water temperature were obtained in several raw and processed formats and therefore had to be carefully checked for congruence. After sorting out any illogical values that have arisen due to the insertion or retrieval of the measuring instruments, calculated average daily values for each thermistor were calculated from the two or four hourly measurements. Subsequently, the measurement series were analysed and tested for completeness in order to select the thermistor with the longest recording for each lake for further calculations.

Id	Name	Date		Total	Days		# of used thermistor
		Start	End		Missing abs.	Missing %	
14	Lungauer Klaffersee	24.08.98	23.09.99	395	0	0.0	1
22	Oberer Landwiersee	09.09.98	07.09.99	363	0	0.0	1
33	Unterer Giglachsee	05.09.98	10.08.03	1800	411	22.8	1
42	Weissensee	28.08.98	31.08.99	368	0	0.0	2
43	Wildlochsee	11.09.98	10.08.03	1794	448	25.0	2

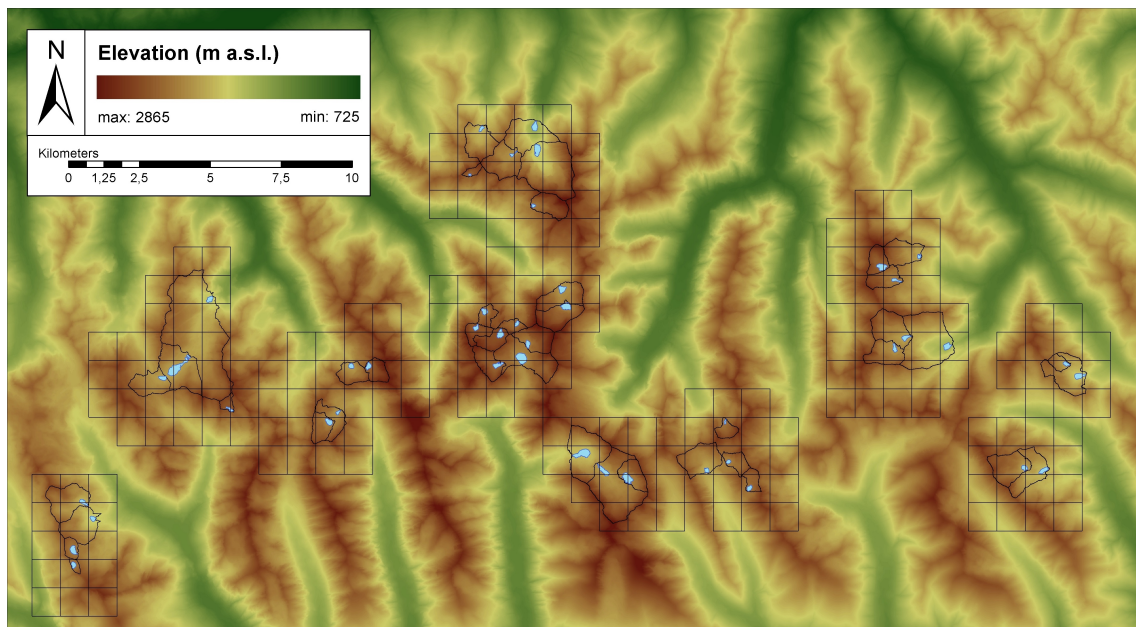
**Table 3.1:** Some statistics about the lakes with missing data.

Table 3.1 provides an overview of the information on the lakes including values, illustrating the measuring period, missing days in absolute numbers and percentage as well as the identification number of the used thermistor. A complete table with all examined lakes can be found in Appendix A on page 53.

As already explained in Chapter 2, after September 1999, there are no longer any measured data for Lungauer Klaffersee, Oberer Landwiersee and Weissensee, which corresponds to an observation period of slightly more than one year and makes meaningful further processing redundant. The lakes Lungauer Klaffersee, Oberer Landwiersee and Weissensee are therefore excluded from the analysis. Furthermore Table 3.1 identifies data gaps for Oberer Giglachsee and Wildlochsee, but the total observation period is still well over 3 years. Considerations to generate the temperature of these lakes by correlating them with up- or downstream lakes with available data were made, but eventually discarded; there was not only a very low correlation between the lakes but also the significance of the results did not greatly increase when including. Therefore the lakes Oberer Giglachsee and Wildlochsee are included in the analysis.

## Catchment delineation

One of the first steps involved the utilisation of the geographic information system software *ArcGIS* to delineate the individual catchments. The elevation data was delivered by the federal states in form of four datasets. The federal state of Styria provided one large .txt file and Salzburg delivered three .tif files. In order to handle the large bulk of data, the .txt files of more than 20 GB was first split up in smaller files of roughly 150 MB each. Afterwards, *LAStools*<sup>1</sup> was used to transform the files into .las format, which is a file type specifically designed for LiDAR data. In the next step, *ArcGIS* was used to generate five .tif files from the .las data, which covered the Styrian part of the research area. Finally, the *Mosaic To New Raster* tool was applied to all raster datasets to obtain one coherent raster for the whole region. Figure 3.1 shows the final DEM and the 44 lakes as polygons, which were created with the help of a hillshade image.



**Figure 3.1:** DEM of the research area with lake/catchment polygons and used SPARTACUS cells

In the next step, the boundaries of the catchment areas were delineated in *ArcGIS* with the help of the DEM and the coordinates of the lake outflows. For this purpose, some basic tools were used to define the flow direction of each grid cell and to check the data set for possible sinks. Then, a stream network was created by means of flow accumulation. By linking the lake outflows to the stream network, I defined the regions upstream of the lake outflows that contribute to surface runoff. These catchment areas, which can be seen in Figure 3.1, were then numbered in alphabetical order according to the corresponding lake and saved as polygons for further processing. Then 50 m contour lines (see Figure 3.2) required for approaches II and III were extracted from the DEM and intersected with the catchment polygons.

<sup>1</sup>software suite with tools for LiDAR data processing

## Air temperature and precipitation data

Due to the fact that there are no hydrological or meteorological measuring stations located directly within the project area, spatially interpolated data of SPARTACUS provided by the ZAMG was used. With the help of *ArcGIS*, the SPARTACUS shapefile is overlapped with the polygons of the catchment areas in the first step. Based on the original idea to explain the LSWT using the air temperature lapse rate, multiple grid cells had to be available per basin to allow for the lapse rate to be calculated. However, the overlaps showed that the grid cells of the data set with an extension of 1 x 1 km were so large that some catchment areas were covered by only one cell, ergo, no lapse rate could be calculated. In order to map the small catchment areas as accurately as possible and at the same time to use sufficient raster data for a reliable statement about the micro-climatic conditions, the catchment areas were therefore divided into two groups:

- five or more raster cells with a direct area share in the catchment area
- less than five raster cells with an area share of the catchment area

For the catchment areas of the second group, the catchment area outline was extended by a buffer of 1 km to include additional grid cells.

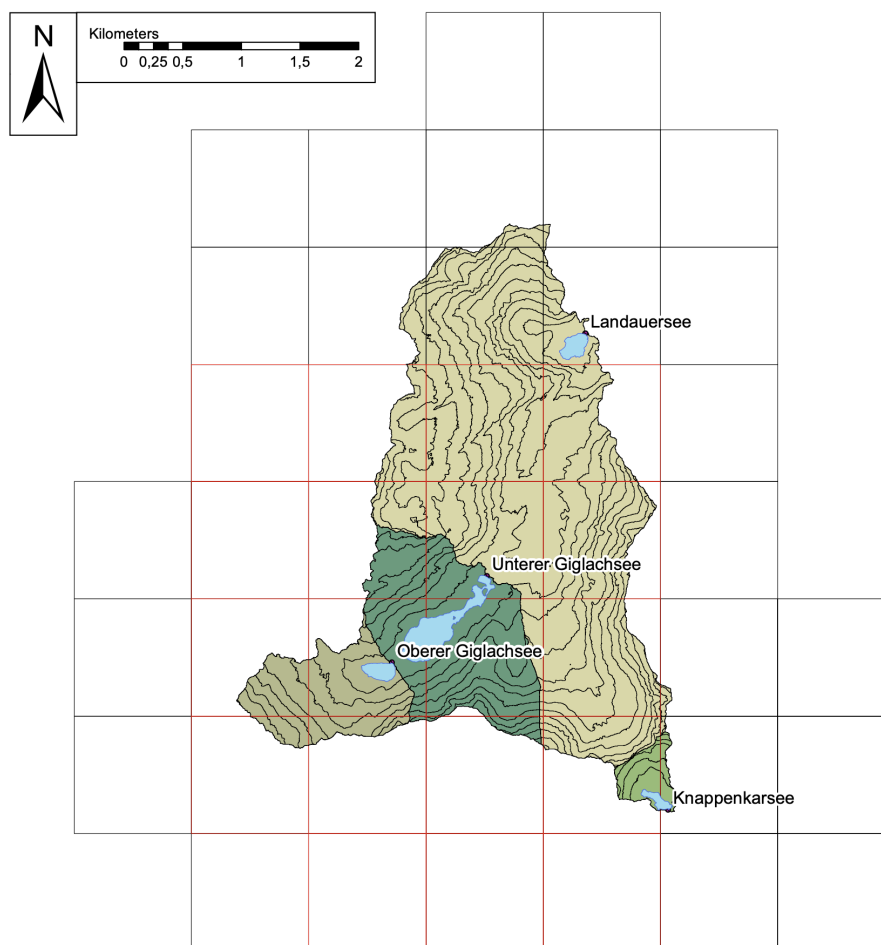


**Figure 3.2:** Close-up of 50 m elevation steps within each catchment and used SPARTACUS cells for Knappenkarsee, Landauersee, Oberer Giglachsee and Unterer Giglachsee (marked red).

Figure 3.2 shows the used SPARTACUS cells for Knappenkarsee, Landauersee, Oberer Giglachsee and Unterer Giglachsee, while all selected grid cells of the SPARTACUS dataset can be seen in Figure 3.1. Subsequently, the mean daily temperature for each grid cell was calculated with the SPARTACUS raw data on the temperature. To smooth out the influence of extreme temperature events, the daily mean temperature was then calculated from the daily minima and maxima for every raster cell (McCombie, 1959). The daily lapse rate could then be calculated for each catchment area by fitting a linear regression to the grids' temperature values and the corresponding mean terrain height of the grids. For the lake classification (see Section 3.2), the mean air temperature lapse rate for the summer months June, July, and August (JJA hereafter) was additionally calculated for all catchment areas, resulting in  $-4.61 \text{ K km}^{-1}$  compared to  $-6.25 \text{ K km}^{-1}$  in the study by Thompson et al..

## 3.2 Lake temperature classification

A great part of the data analysis and modelling process is determined by the classification of the lakes into groups based on their average summer water temperature. What may look like a straightforward procedure imposed some difficulties, which are discussed in the following subsections.

### Previous research

Thompson et al. (2005) introduce a classification into five groups by correlating the lakes' average summer water temperatures and altitudes with an expected rate of change in air temperature with the elevation for the summer months JJA ( $-6.25 \text{ K km}^{-1}$ ), which can be seen in Figure 3.3. Therefore, six lakes are classified as unusually cold, four lakes as cool, 26 lakes as average, six lakes as slightly warmer than the average and three lakes as unusually hot.

The attempt to reconstruct the lakes' average summer water temperatures on the basis of raw data yielded significantly different results. As Thompson et al. lacked the exact definition of the summer months used for the calculation, various combinations of months were tested. As Thompson et al. lacked the exact definition of the summer months used for the calculation, various combinations of months were tested, the results of the thermistor averages for each month can be found in the first three figures of Appendix B from page 59 on. In June, mean water temperatures are significantly colder than those of the previous classification. The mean values of July are most similar to those of the previous classification, but nonetheless do not match. In August it can be seen that the calculated water temperatures are significantly warmer than the values of the previous study. In addition, the water temperatures were calculated for the mean value of both thermistors as well. Nonetheless, the original values of the average summer water temperature could not be reproduced.

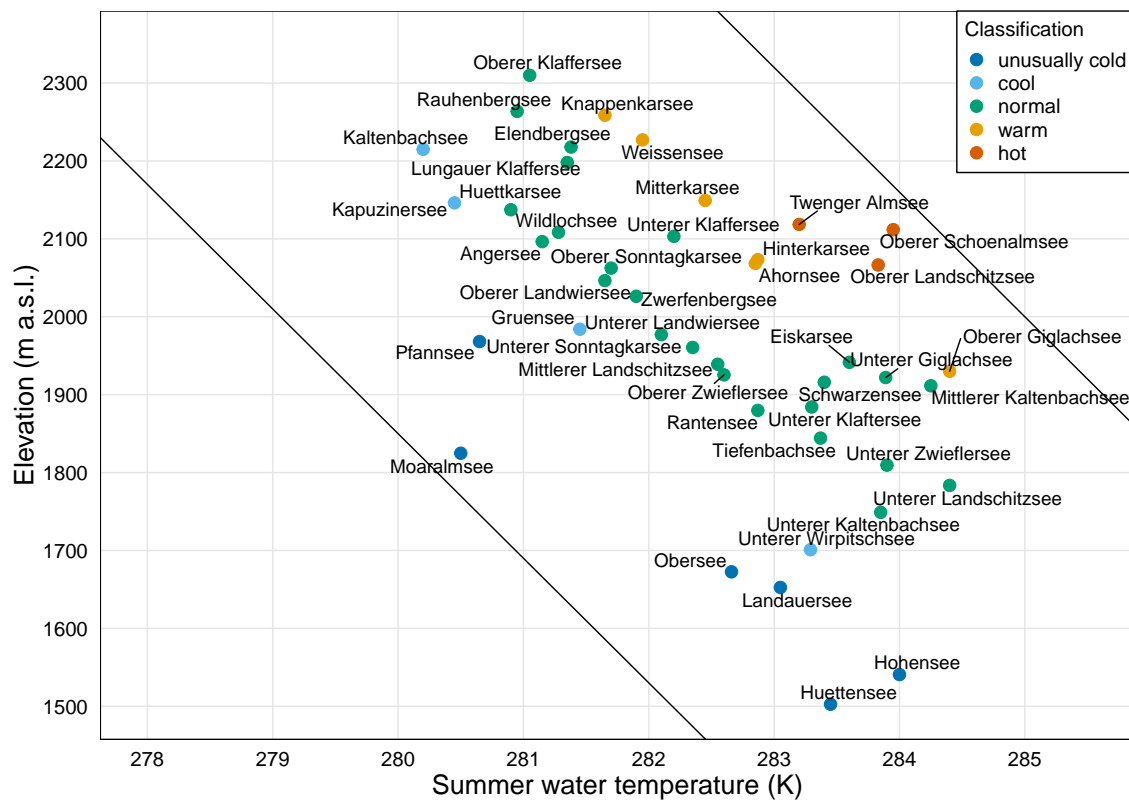


**Figure 3.3:** Classification based on paper by Thompson et al. (2005), with the diagonal lines displaying the air-temperature lapse rate.

## Present data

As a result of the inconsistency, the need to introduce a new classification for the dataset emerged. In terms of the thermistor that was used for calculating the average summer water temperature, the one with the longest measuring time per lake was selected for each lake (see Table A.1 in Appendix A on page 53 for selected thermistors). Figure B.4 in Appendix B on page 61 illustrates the differences of Thompson et al. and the current data set. Here, the offsets are represented by horizontal lines, with small dots representing the original values from the paper by Thompson et al. and bold dots signifying the calculated values from the received data set. The color scale and lapse rate diagonals are based on Thompson et al. (2005). In general, the majority of the lakes at higher altitudes show significantly colder mean water temperatures than previously reported. On average, the temperature of lakes above 1,950 m a.s.l. decreases by -0.9 K, and in the case of Oberer Landwiersee the temperature decreases even by 2.5 K. The lower lakes, however, show an increase in mean water temperature compared to the original study. Thus, the mean water temperature of lakes lower than 1.950 m a.s.l. increases by 0.5 K on average. Unterer Kaltenbachsee and Hohensee even show a rise of 1.4 K.

All results and the classification by temperature can be found in Appendix A in the Table A.3 on page 56. Figure 3.4 shows the altitude of the lakes and their calculated average summer water temperature for JJA, which were defined as summer months as they have

the highest air temperature. The diagonal lines represent the mean air temperature lapse rate of these summer months in the project area whose gradient is  $4.61 \text{ K km}^{-1}$ . Based on a parallel shift of these diagonals, the lakes were divided into temperature classes. As already mentioned, the original division into five classes was not reasonable, this approach is discontinued here. Instead, the grouping is reduced to three classes with each one taking up one third of the area between the two diagonal lapse rate lines.

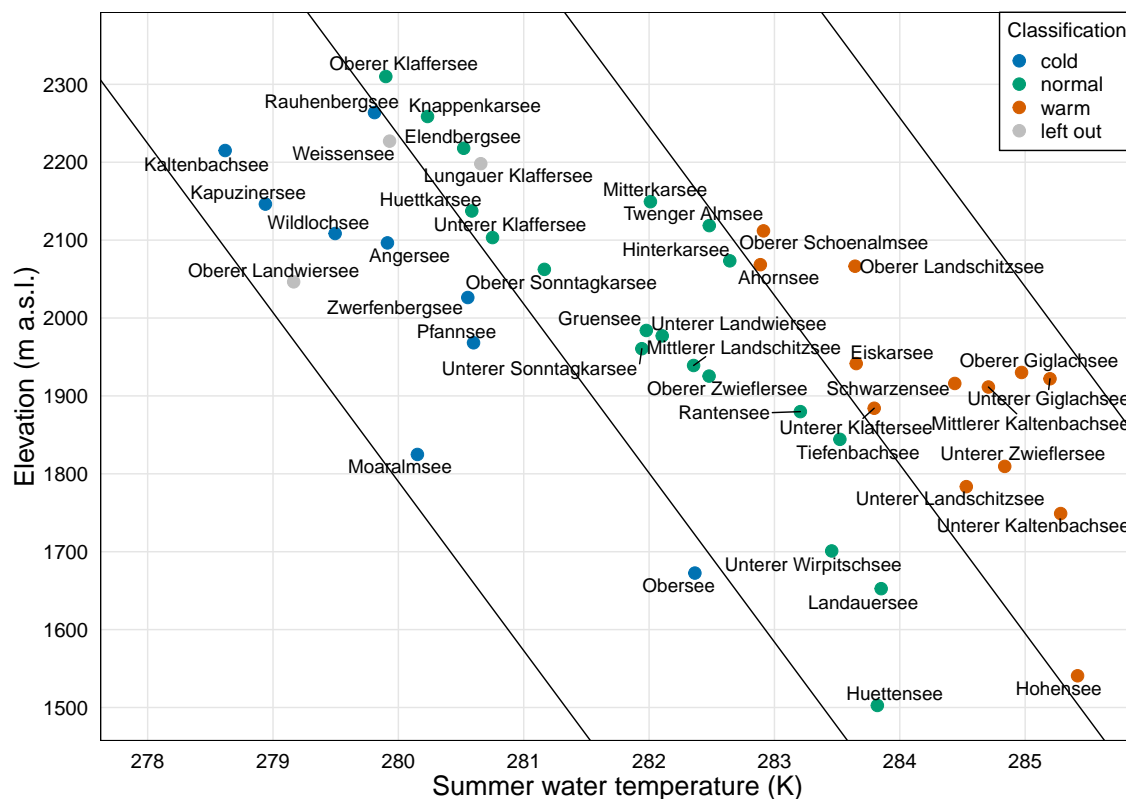


**Figure 3.4:** Classification based on received data, with the diagonal lines displaying the air-temperature lapse rate calculated with SPARTACUS data.

This classification now yields 9 cold, 19 normal, and 13 warm lakes (see Table A.3 for details). A comparison of this new classification with the Thompson et al. definition shows clear differences.

Following the new classification and grouping the lakes of the previous study in three similar categories (unusually cold and cool as cold; normal; warm and hot as warm), one would change 21 of the lakes into another category. Lake Hohensee stands out as it is the only one that falls into the opposite class, i.e. from unusually cold to warm. The remaining 20 lakes keep their previous class.

This classification serves as a reference point for the following approaches.

### 3.3 Approaches

The different approaches are presented in detail in the following three sections, where the underlying formulas will be explained.

## Approach I – Catchment topography

As a first step to understand the temperature anomalies of the studied lakes, the elevation distributions of the catchments is examined. Based on the assumption that the water temperature of a lake is largely dependent on the diffuse inflow from the respective catchment area, information on the thermal characteristic of the lake can be derived from the topography of the catchment area itself. Hence, lakes with a lower than average water temperature should have more shares of their catchment area in higher elevated areas, and colder water from precipitation events or snow melt would drain into them. In the opposite case, lakes with a comparatively high water temperature should have more parts of their catchment area in lower-lying areas, so generally warmer water from precipitation events and less snow melt would flow into them. In order to verify this hypothesis, four groups are formed as shown in Figure 3.5, each containing at least one lake classified as cold, normal and warm classified lake in a range of 50 m in altitude. The lakes of the first group are Angersee, Wildlochsee, Twenger Almsee, Unterer Klaffersee and Schoenalmsee and lie between 2,135 and 2,085 m a.s.l.. Those of the second group are Zwerfenbergsee, Oberer Sonntagkarsee, Ahornsee and Oberer Landschitzsee and are located between 2,070 and 2,020 m a.s.l.. The third group is ranging from 1,980 to 1,930 m a.s.l. and consists of Pfannsee, Mittlerer Landschitzsee, Unterer Landwiensee, Unterer Sonntagkarsee, Eiskarsee and Oberer Giglachsee. Moaralmsee, Tiefenbachsee and Unterer Zwieflersee form the fourth group and are located between 1,855 and 1,805 m a.s.l..

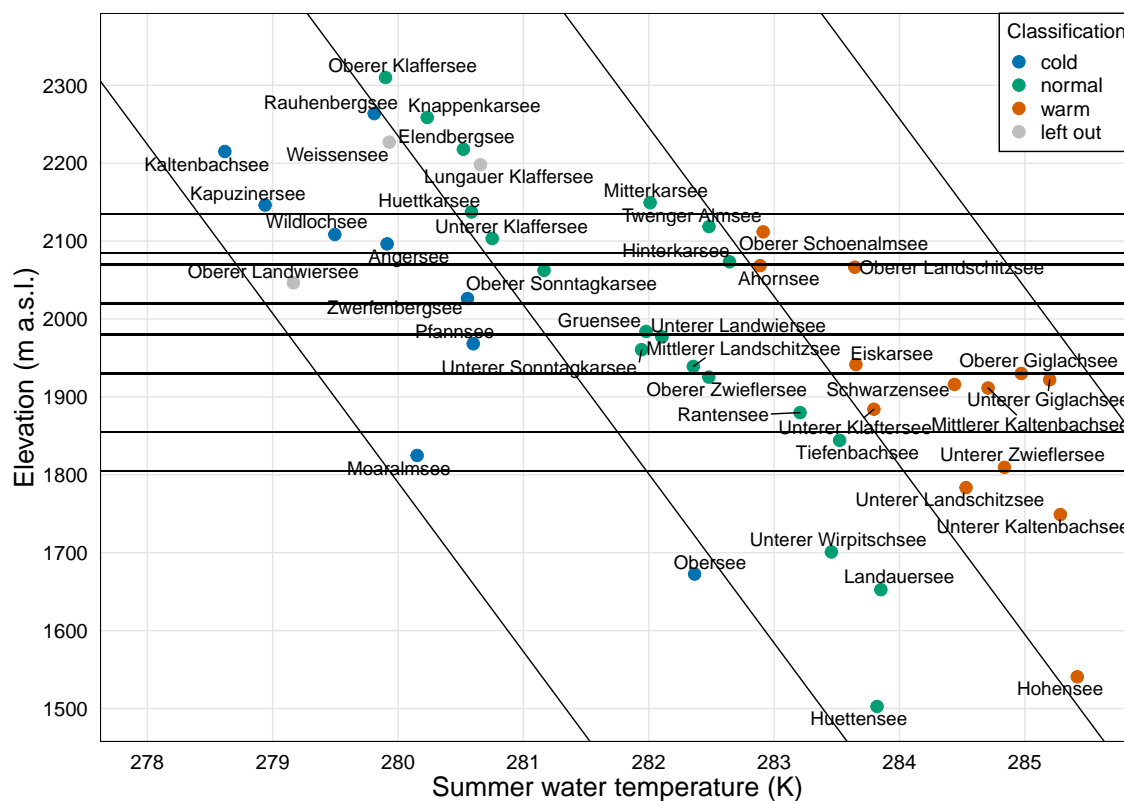


Figure 3.5: Limits and numbering of lake groups

The software *ArcGIS* was used to extract the elevation data of the catchment areas from the DEM of the study area. In the next step, the density distribution curves of all catchment areas of the respective groups were created and processed using *R*. Each group figure illustrates the elevation distribution as a percentage of the catchment areas and thus provides information about their topographic characteristics. The resulting plots can be found in section 4.1; all additional plots are included in Appendix A.

## Approach II – Catchment air temperature

Since earlier studies show a close correlation of water and air temperature (see Livingstone et al. (1999); Edinger et al. (1968); Piccolroaz et al. (2013)), the second approach compares the mean air temperature of the catchment areas with the mean water temperature of the lakes for the summer months of JJA to evaluate a potential relationship between those two.

More precisely, the average summer air temperature of the respective catchment areas is compared with the classification of the lakes according to their average summer water temperature. If this results in a similar distribution, this would indicate that the differences in water temperature may possibly be explained by the different thermal conditions within the catchment areas. In order to represent these individual micro-climatic conditions as precisely as possible with the available data, an air temperature lapse rate is calculated for each catchment area using the corresponding SPARTACUS cells, which is then further used to calculate the catchments average air temperature by taking the topography into account. As already explained in section 3.1, the necessary grid cells are selected using the catchment polygon. By contrast, for catchments with less than five grid cells, a buffer of 1 km is added in order to obtain more cells for the analysis. Since the mean height of each grid cell is known, a daily lapse rate of the air temperature can be calculated for each catchment by fitting a linear regression to the data with *lm*-function in *R*. This calculates a regression by the method of ordinary least squares as displayed with Equation 3.1, where  $\alpha$  and  $\beta$  stand for the regression parameters (gradient and intersection with y-axis) and  $X_i$  for the mean terrain height of the grid cell.

$$f(X_i, \alpha, \beta) = \alpha_{airtemp} + \beta_{airtemp} X_i \quad (3.1)$$

In the next step, the catchment areas are divided into 50 m elevation layers, the mean terrain height of which is expressed as  $x_i$ , and their respective area (defined as  $A_{x_i}$ ) is calculated. The mean air temperature of each watershed can then be calculated using Equation 3.2.

$$f(x_i, \alpha, \beta) = \sum_{i=1}^n \frac{(\alpha_{airtemp} + \beta_{airtemp} x_i) * A_{x_i}}{\sum A_{x_i}} \quad (3.2)$$

This calculates the air temperature for each elevation zone and weighs it according to

its share in the total catchment area. The average air temperature for each catchment area is then determined by calculating the mean value of all daily values over the summer months JJA. The average summer air temperature can then be represented in the same way as the water temperature, i.e. in relation to the lakes' elevation level. Using the same color classification introduced in Figure 3.4, the relative position of the lakes can now be compared.

### Approach III – Catchment energy input

Approach III includes the precipitation information from SPARTACUS in the analysis. Using the data on the sum of the daily precipitation and the mean daily air temperature, I calculated an energy balance of the catchment areas. Following the same patterns as in approach II, I firstly calculated a daily lapse rate for each catchment area, i.e. an elevation dependent ratio of precipitation (see Equation 3.1). Then, in Equation 3.3, the 50 m altitude layers are used to compute the precipitation and temperature for each zone and weigh according to their share of the total area of the catchment area.

$$f(x_i, \alpha, \beta) = \sum_{i=1}^n \frac{(\alpha_{airtemp} + \beta_{airtemp}x_i) * \max(\alpha_{precip} + \beta_{precip}x_i, 0) * A_{x_i}}{\sum A_{x_i}} \quad (3.3)$$

In contrast to approach II, if precipitation is present, it is now multiplied by the air temperature to obtain an energy unit in form of K mm m<sup>-2</sup>. This value is calculated as the average yearly mean for the summer months of JJA as well as for the remaining months of the year (September to May) and then compared.

Since this approach is restricted to the total energy input, I additionally created a variation of Equation 3.3 (see Equation 3.4), where only precipitation on days with an average air temperature below 273.15 K is included in the calculation. This equation should therefore represent the snowfall within the catchment areas and is examined as the yearly average sum for the summer months and the remaining year.

$$f(x_i, \alpha, \beta) = \sum_{i=1}^n \frac{\min(\alpha_{airtemp} + \beta_{airtemp}x_i, 273.15) * \max(\alpha_{precip} + \beta_{precip}x_i, 0) * A_{x_i}}{\sum A_{x_i}} \quad (3.4)$$

## 4. Results and discussion

This chapter presents and describes the results of the three approaches. Subsequently, these findings are evaluated in the following discussion and then critically assessed in a scientific context. Finally, perspectives on possible further directions are given.

### 4.1 Approach I – Catchment topography

#### Results

The results of the first approach are visualized on the following pages for the four groups defined in Figure 3.5 on page 27. This following color scheme applies to all figures: lakes classified as cold are shown in blue, those classified as normal in green and those classified as warm in red. The scale of the x-axis (elevation m a.s.l.) is constant in all figures, only the values of the y-axis (the percentage of the total catchment area) vary. The display of the raster data on the elevation information was divided into 10 meter increments so that differences can be visually identified. Otherwise, the high resolution of the DEM would have resulted in lower percentage values, where the data series of the catchment areas with a dominant altitude zone would have been difficult to display. If one integrates the area below the curve, the result is 100%. While the elevation density distribution of the different catchment areas is shown as curves with different colors and line types, vertical lines show the average elevation of the respective catchment areas. Further parameters concerning the landcover of all catchments can be found in Table A.2 in Appendix A on page 55. The elevation density distributions of the other lakes, which are not part of a group, are shown in Figure 2.

#### Group 1

Figure 4.1 shows the distribution of the height density of the catchment areas of the first group with the highest elevated lakes. It includes the two lakes Angersee and Wildlochsee, which are classified as cold and depicted in blue, where the lake is located at an elevation of 2,096 m a.s.l. and 2,109 m a.s.l. respectively. Their highest points within the catchment areas are at 2,702 m a.s.l. (Angersee) and 2,747 m a.s.l. (Wildlochsee). The lakes marked in green, i.e. classified as normal temperate, are the Twenger Almsee and Unterer Klaffersee, which lie at 2,119 m a.s.l. and 2,103 m a.s.l.. The highest point of the catchment area in these cases is at 2,319 m a.s.l. (Twenger Almsee) and 2,379 m a.s.l. (Unterer Klaffersee). The only warm classified lake of the group, the Oberer Schoenalmsee, located at 2,112 m a.s.l., is displayed in red. Its highest point within the catchment area is at 2,328 m a.s.l..

Considering the elevation distribution of the differently classified lakes, one can see

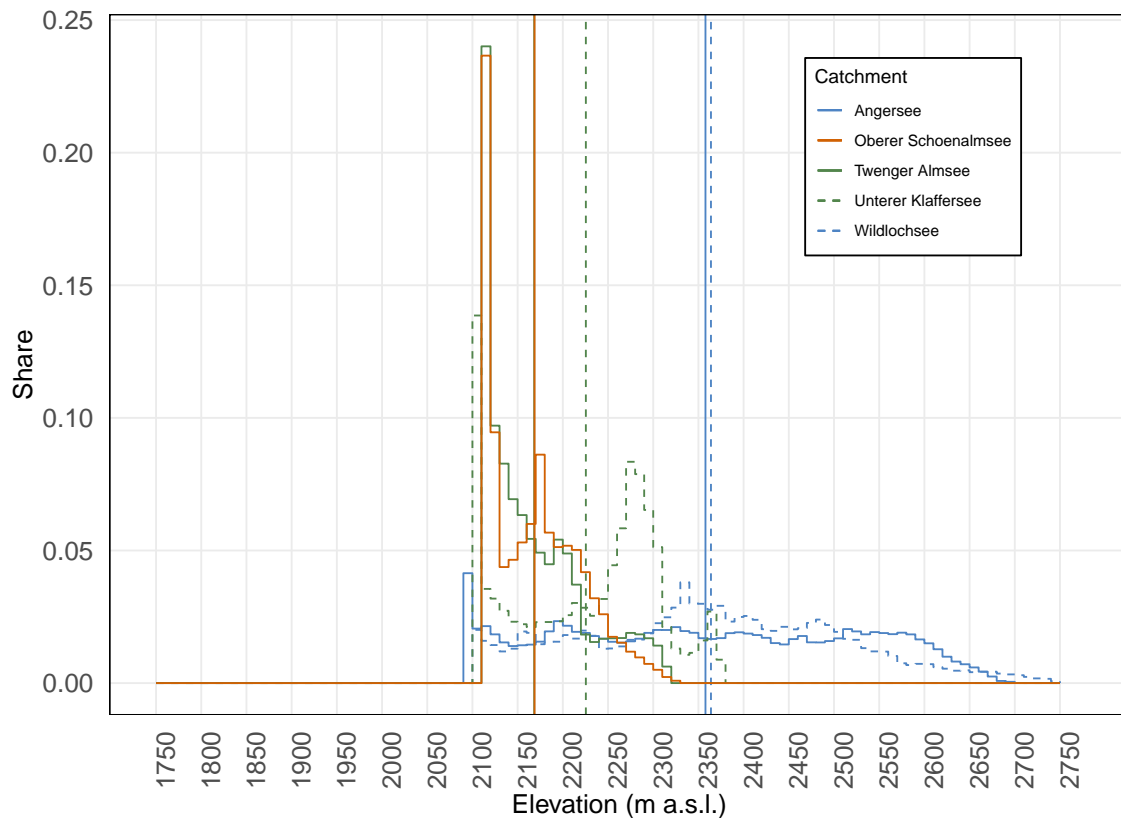


**Figure 4.1:** Group 1: Elevation density distribution of Angersee, Wildlochsee, Twenger Almsee, Unterer Klaffersee and Oberer Schoenalmsee

that the lakes classified as cold are the only lakes in this group that also have shares in their catchment area above 2,380 m a.s.l.. Moreover, the shape of their distribution curves is very similar in comparison. With regard to Angersee, the curve has a rather constant shape, i.e. the catchment area is evenly distributed over the altitudinal range. Consequently, no dominant altitude zone can be identified, with the highest part of the catchment area being the lake itself at approximately 2,095 m a.s.l.. The Wildlochsee has the largest part of its catchment area at an altitude of around 2,335 m a.s.l.. Above that, the curve gradually drops flat. Similar to the first lake classified as cold, no dominant altitude zone could be identified. The average altitudes of the two catchment areas are also close to each other; for Angersee it is 2,358 m a.s.l. and for Wildlochsee 2,364 m a.s.l.. The normal classified Unterer Klaffersee displays a peak at 2,105 m a.s.l. defining the surface area of the lake itself and another one at about 2,280 m a.s.l.. These two elevation zones represent the largest part of the catchment area with 14 percent of its share at the first peak and about 17 percent at the second peak between 2,270 to 2,290 m a.s.l.. In comparison, the areas between the two peaks and above the second one represent a rather small part of the entire catchment area. The mean altitude of the Unterer Klaffersee watershed lies in the center of the five catchment areas of the group at 2,225 m a.s.l.. For the second normal classified Twenger Almsee a right-skewed distribution can be observed. Its dominant elevation zone is located at 2,115 m a.s.l. representing about 24 percent of the whole catchment area. The curve then steeply

drops to around 5 percent at 2,200 m a.s.l. and then further to 2 percent at 2,300 m a.s.l. The mean altitude of this catchment area is 2,168 m a.s.l., which is similar to that of the warm classified Oberer Schoenalmsee at 2,169 m a.s.l.. Besides that, the distribution curve itself strongly resembles that of the Twenger Almsee, with a dominant peak of about 24 percent at 2,110 m a.s.l. and another small peak (9 percent) at 2,175 m a.s.l..

## Group 2

Figure 4.2 displays the elevation density distribution of the second group of catchments. This group consists of the cold classified Zwerfenbergsee, the normal classified Oberer Sonntagkarsee and the two warm classified lakes Ahornsee and Oberer Landschitzsee. The Zwerfenbergsee at 1,810 m a.s.l. is the lake at the lowest altitude, whereas its catchment area is the second highest in the group with a maximum elevation of 2,614 m a.s.l.. Only the catchment area of the Oberer Sonntagkarsee is higher, with a maximum height of 2,702 m a.s.l., whereby the lake here is the second lowest at 2,112 m a.s.l.. With 2,067 m a.s.l., Oberer Landschitzsee is the second highest lake in the group, but its catchment area is the lowest with a maximum elevation of 2,476 m a.s.l.. The catchment area of the highest elevated lake in the group (2,069 m a.s.l.), the Ahornsee, extends to 2,522 m a.s.l..

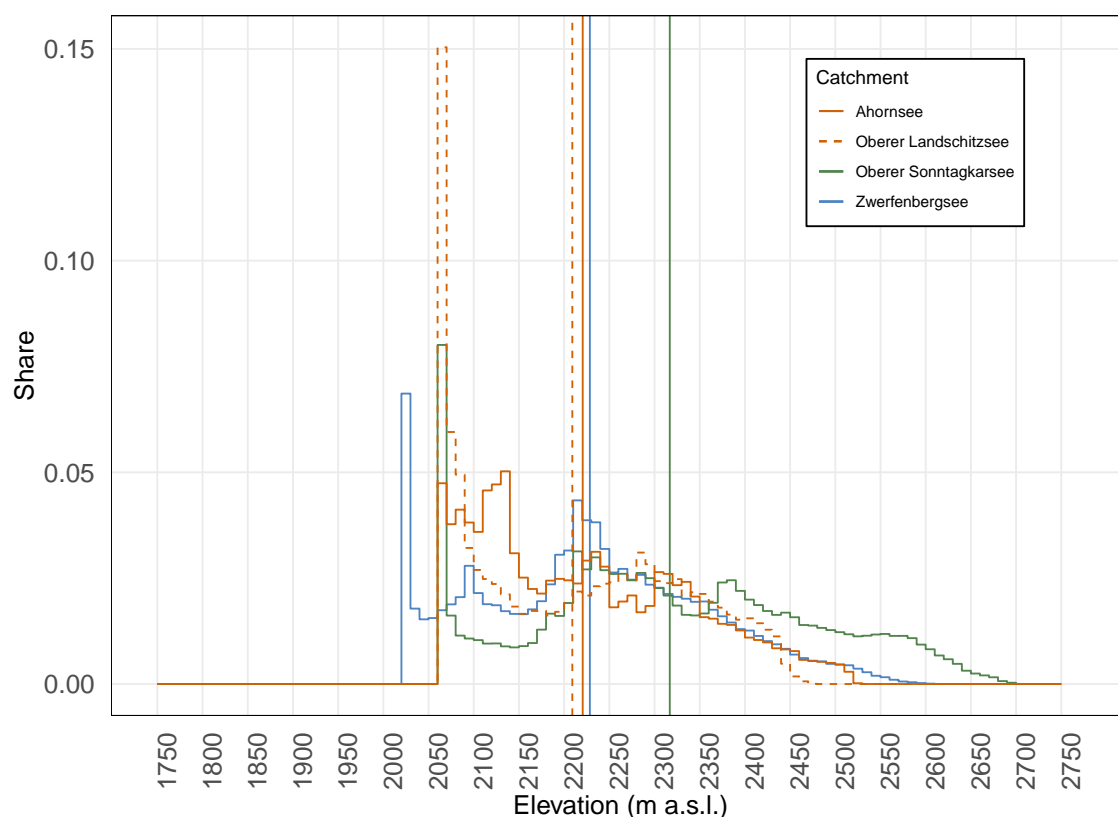


**Figure 4.2:** Group 2: Elevation density distribution of Zwerfenbergsee, Oberer Sonntagkarsee, Ahornsee and Oberer Landschitzsee

Two prominent peaks emerge with regard to the cold classified Zwerfenbergsee.

These mark the largest shares of the catchment area in the altitude zones of 2,025 m a.s.l. and account for about 7 percent and 2,220 m a.s.l. with a share of about 4 percent. In the center of the two peaks is another local maximum with roughly 2.5 percent at 2,095 m a.s.l., whereas the curve decreases steadily after the second peak. The mean height of the catchment area is 2,229 m a.s.l., positioned almost at the same level as the second peak. The largest part of the catchment area of the normal classified Oberer Sonntagkarsee are the areas at 2,065 m a.s.l., which account for about 5 percent of the watershed area. The share of higher elevated areas up to 2,160 m a.s.l. is comparatively low at around 1 percent. After that, the percentage abruptly rises up to 2,225 m a.s.l. and then slowly falls again. With 2,317 m a.s.l., this watershed has the highest average altitude compared to the other catchment areas of the group. The elevation density distribution of the Oberer Landschitzsee shows one prominent peak at 2,070 m a.s.l., accounting for 15 percent of the catchment area, and steeply falls with increasing elevation. A much smaller local maximum of a 3 percent share is located at the altitude zone of around 2,285 m a.s.l., where the curve descends to both sides. The mean catchment height is the lowest of the group and is located at 2,209 m a.s.l., approximately halfway between the two above-mentioned peaks. The mean catchment height of Ahornsee, the second lake classified as warm, is 2,221 m a.s.l. and thus lies between Oberer Landschitzsee and Zwerfenbergsee. Its density distribution curve shows two smaller peaks with 5 percent share of the catchment area at 2,055 m a.s.l. and 2,125 m a.s.l. In the further course the curve has a rather descending course with two smaller peaks of half the percentage at 2,230 m a.s.l. and 2,320 m a.s.l..

### **Group 3**

The results of group 3 are exemplified in Figure 4.3. In this group, there is one lake, the Pfanensee, classified as cold, three normal classified lakes (Mittlerer Landschitzsee, Unterer Landwiersee and Unterer Sonntagkarsee), and two warm classified lakes (Eiskarsee and Oberer Giglachsee). The Pfanensee is located at 1,968 m a.s.l. and therefore the second highest elevated lake of the group, while its catchment area extends to a maximum elevation of 2,542 m a.s.l.. The Mittlerer Landschitzsee is located at an altitude of 1,939 m a.s.l. and its catchment area extends to 2,727 m a.s.l., making it the highest ranging within the group. As the highest elevated lake, Unterer Landwiersee is located at 1,977 m a.s.l., but the maximum elevation of its catchment area is 2,480 m a.s.l., which is in the mid-range of the group. The third normal classified Unterer Sonntagkarsee is located at 1,961 m a.s.l. and has the second highest ranging catchment area with 2,583 m a.s.l.. Lake Eiskarsee is located at 1,942 m a.s.l. and its catchment area extends to 2,462 m a.s.l.. With 1,930 m a.s.l. the lowest elevated lake of the group and with 2,304 m a.s.l. also the catchment area with the lowest maximum elevation, the Oberer Giglachsee completes the group.

The curve of the cold classified Pfanensee has a crown-like course with three maximum

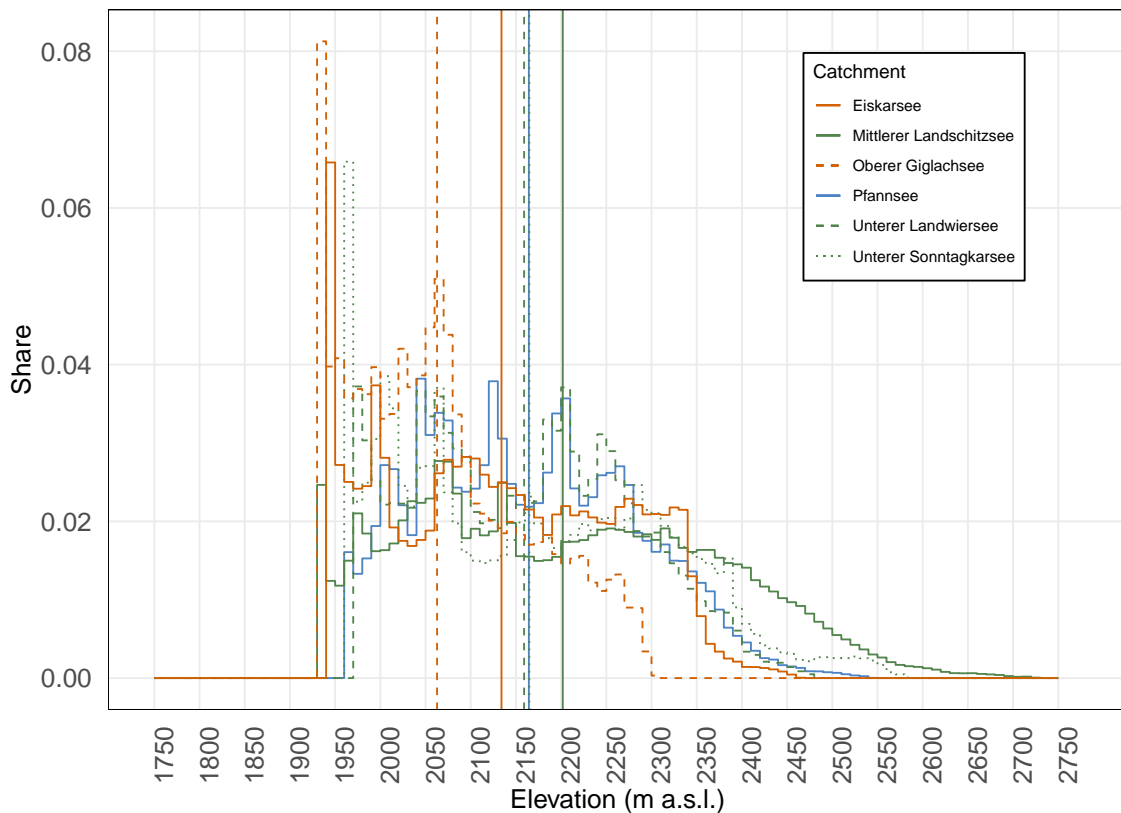


**Figure 4.3:** Group 3: Elevation density distribution of Pfanensee, Mittlerer Landschitzsee, Unterer Landwiersee, Unterer Sonntagkarsee, Eiskarsee and Oberer Giglachsee

peaks of an areal catchment share of around 4 percent at 2,050 m a.s.l., 2,125 m a.s.l. and 2,200 m a.s.l.. In addition, two local maxima at 2,010 m a.s.l. and 2,265 m a.s.l. with about 3 percent share and the mean elevation of the catchment area at 2,164 m a.s.l. can be observed. Two of the three curves of the normal classified lakes, Unterer Landwiersee and Unterer Sonntagkarsee, are similar to those of Pfanensee, as both have multiple local and global peaks. For instance, in addition to the three maximum peaks at 1,975 m a.s.l., 2,065 m a.s.l. and 2,205 m a.s.l., the curve of Unterer Landwiersee has one smaller peaks at 2,245 m a.s.l. prior to a stark drop of the curve. At Unterer Sonntagkarsee, one major peak at 1,965 m a.s.l. with more than 6.5 percent areal catchment share and two smaller peaks with around 4 percent each at 2,005 m a.s.l. and 2,065 m a.s.l. can be noticed. In the further course of the curve, the drop is rather slight but indicates three small spikes at 2,165 m a.s.l., 2,285 m a.s.l., and 2,385 m a.s.l.. The curve of the third lake, Mittlerer Landschitzsee, which is classified as normal, is flatter and has less pronounced peaks in comparison to the two previous ones. In terms of surface area, the height zone of 2,070 m a.s.l. accounts for the largest share of the catchment area, while the zones from 1,940 to 2,060 m a.s.l. and 2,080 to 2,320 m a.s.l. account for a similarly large share, averaging about 2 percent. At 2,202 m a.s.l., the Mittlerer Landschitzsee has the highest average elevation of the catchment area of the entire group, whereas the two other lakes classified as normal are in a similar range as Pfanensee at 2,159 m a.s.l. (Unterer Landwiersee) and 2,165 m a.s.l. (Unterer

Sonntagkarsee). The curve of the Eiskarsee, classified as warm, is right-skewed and has its maximum of about 6.5 percent at 1,945 m a.s.l.. In its further course it drops down again to a local maximum of less than 4 percent at 1,995 m a.s.l.. Subsequently, a uniformly downward sloping plateau can be seen from about 2,090 to 2,340 m a.s.l, after which the curve drops off steeply. The mean height of this catchment area is 2,134 m a.s.l. and thus below that of the lakes classified as normal and cold, but far above that of the second lake classified as warm at 2,063 m a.s.l. (Oberer Giglachsee). The height density distribution of this catchment area shows two prominent maxima, one with an 8 percent areal share at 1,935 m a.s.l. and another one with a 5 percent share at 2,065 m a.s.l.. Averaging the elevation range between these peaks, one gets a mean percentage of about 4. After the second peak, the curve drops first steeply and then flat until it drops steeply again from 2,270 m a.s.l. on.

#### **Group 4**

The elevation density distribution of the three lakes of group 4 and therefore the lowest elevated lakes is pointed out in Figure 4.4. Here, one lake of each category is analysed. The Moaralmsee, which is classified as cold, is located at 1,825 m a.s.l. and the maximum elevation within its catchment area is found at 2,537 m a.s.l. making it the highest ranging watershed within group 4. Above the Moaralmsee, the normal classified Tiefenbachsee lies at 1,844 m a.s.l., whose catchment area is the lowest ranging with a maximum of 2,410 m a.s.l.. The Unterer Zwiefeldersee is classified as warm at 1,810 m a.s.l., making it the lowest lake in the group, while its catchment area reaches up to the elevation of 2,441 m a.s.l..

Moving on to the last figure of the first approach, it can be seen that the density curve of the Moaralmsee, which is classified as cold, has a prominent peak at 1,845 m a.s.l., which represents about a 5 percent share in the area of the corresponding catchment. In the further course of the curve, it first drops steeply until two local maxima at 1,975 m a.s.l. (3 percentage) and 2,035 m a.s.l. (2.5 percentage) are reached. After that, the curve drops slowly, from 2,200 m a.s.l. onwards, it becomes steeper for the next 200 meter and then flatter again. The mean height of the catchment area is 2,034 m a.s.l., which is between those of Unterer Zwiefeldersee (1,994 m a.s.l.) and Tiefenbachsee (2,069 m a.s.l.). The graph of the Tiefenbachsee, classified as normally temperate, shows a more diverse course than the one of the Moaralmsee. In addition to the global maximum marking a share of 4.5 percent at 2,115 m a.s.l., there are three more local maxima in descending order at 2,015 m a.s.l., 1,845 m a.s.l. and 1,955 m a.s.l.. Besides the two local minima with approximately equal shares of the catchment area at 1,975 m a.s.l. and 2,075 m a.s.l., there is also a global minimum at 1,900 m a.s.l. accounting for 1 percent of the catchment area. From 2,220 m a.s.l. on, the graph drops steeply and steadily. The graph of the lowest situated Unterer Zwiefeldersee has a similarly diverse course as that of the Tiefenbachsee. With more than 5 percent, the elevation of 1,855

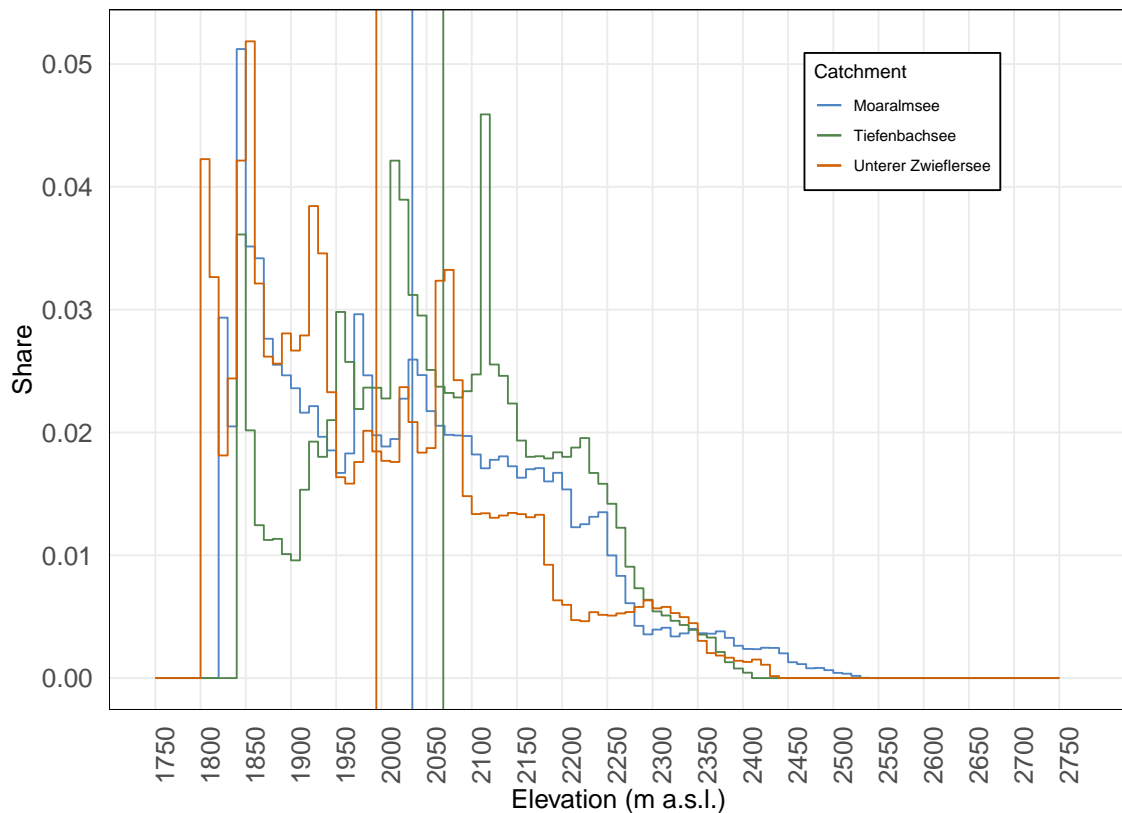


**Figure 4.4:** Group 4: Elevation density distribution of Moaralmsee, Tiefenbachsee and Unterer Zwiefeldersee.

m a.s.l. has the highest share of the catchment area, followed by three further peaks at 1,805 m a.s.l., 1,925 m a.s.l., and 2,070 m a.s.l.. Areas at higher altitudes have only a small share of the catchment area, as the vertical line for the average altitude of the catchment area already indicates.

## Discussion

Comparing the results of the four groups, one can observe that the underlying hypothesis of the water temperature of the lakes being strongly affected by the topography of the catchment area cannot be confirmed. According to this hypothesis, cold lakes should have larger proportions of their catchment areas at high altitudes, from which colder surface runoff then discharges. Conversely, it could be expected that warm lakes have large parts of their catchment areas in low-lying areas so that generally warmer water flows in. For the first group, this thesis can be confirmed and the catchment areas of the two cold classified lakes are significantly higher than the other catchment areas of the group. The catchment area of the warm lake is also significantly lower compared to the other four catchments of the same group. Yet, the figures of the other three groups show a different picture. With regard to the elevation density distribution curves of the cold and normal classified lakes, the initial hypothesis does not hold up and no distinctive features underlying all these curves can be derived. However, the curves of the lakes classified as warm tend to have a larger proportion of their catchment areas in low-lying

areas than the lakes of the other two groups. It is also striking that the largest percentage of the catchment area is at the lowest level of the catchment area, i.e. the lake surface itself has a large share of the catchment area. Comparing this observation with the characteristics of the catchment areas of the other classes, a trend can be observed that the lowest level of the catchment areas of the cold lakes more often makes up a smaller part of the total area than in the lakes classified with another temperature characteristic. Since the initial hypothesis trying to explain differences in water temperature can solely by means of the topography of the catchment areas must be rejected, the next step additionally includes spatially interpolated data on air temperature.

## 4.2 Approach II – Catchment air temperature

### Results

The result of the second approach is visualized in Figure 4.5 which, for the sake of comparability, follows the same scheme as the original classification in Figure 3.4 on page 26. Since this section is limited to the results, the auxiliary Figure B.5, which facilitates a direct comparison of the two figures, is located in Appendix B on page 61. Regarding the data of the average water and air temperature during the summer months, consider Table A.3 in Appendix A. Concerning Figure 4.5, the x-axis shows the mean air temperature of the lake catchment areas for the summer months JJA. The air temperature was calculated using a lapse rate: In a first step, five or more grid cells of the SPARTACUS data set surrounding each catchment area were selected. On the basis of the information on the mean air temperature and elevation of the grid cells taken from the DEM, a daily lapse rate of the air temperature was calculated. This lapse rate was then used to calculate the temperature for the catchment areas divided into 50 m altitude bands. In the last step, a daily mean air temperature of the catchment area was calculated by weighing the respective area share of the altitude bands in the total area of the catchment area. The average of the calculated air temperature is shown on the x-axis. The y-axis signifies for the elevation in meters above sea level, whereby the lakes are plotted in relation to the elevation at which they are located.

Comparing the original Figure 3.4 and Figure 4.5 resulting from approach II, one discovers that the examined lakes, especially at high altitudes, are displayed much closer to each other in the air temperature plot and do not scatter as much within the altitude zones as is the case with the water temperature plot. All cold classified lakes in this plot generally shift to the right, i.e. have a higher mean air temperature than water temperature. For example the average air temperature in the catchment areas of Kaltenbachsee and Moaralmsee during JJA is 276.55 K, which is 3.34 K warmer than the water temperature in the same timespan. In all other cold lakes, the air temperature is at least 1 K above the water temperature. Although the temperature difference is not quite as large when compared to the cold lakes, lakes classified as warm shift to the left, i.e. have comparatively colder air temperatures than water temperatures. Thus, the

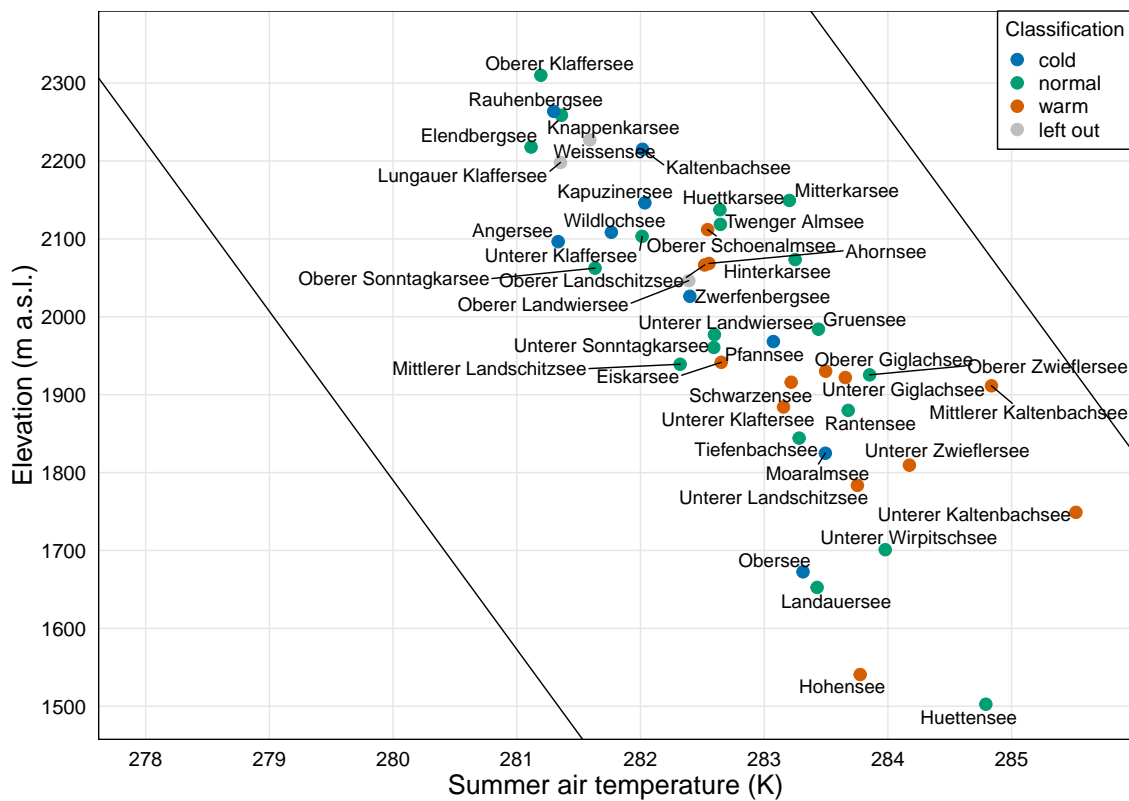


**Figure 4.5:** Average air temperature of each catchment for the summer months June, July and August compared to lake elevation. The diagonal lines displaying the air-temperature lapse rate calculated with SPARTACUS data.

Hohensee water temperature shifts from 285.42 K to 283.78 K air temperature, which is a difference of -1.64 K. Both Oberer Giglachsee and Unterer Giglachsee show similar shifts, of -1.47 K and -1.54 K respectively. With the exception of Mittlerer Kaltenbachsee and Unterer Kaltenbachsee, all other lakes classified as warm also show colder air than water temperature during the summer months. The air temperature in the catchment areas of the lakes classified as normally temperate depicts shifts in both directions but tends to become warmer on average with greater differences between the water and air temperature, particularly in the higher-lying catchment areas.

## Discussion

The results of the hypothesis of the second approach testing whether the respective water temperature of the lakes are strongly dependent on the thermal conditions in the catchment areas are now discussed. According to the initial hypothesis that air and water temperature closely correlate (see Livingstone et al. (1999)), a similar distribution of lakes as in Figure 3.4 would be expected if all of the lakes are largely influenced by air temperature. At the same altitude level, lakes with colder water temperatures would have catchment areas with comparatively cold air temperatures and vice versa. Figure 4.5, however, contrasts with Figure 3.4 and shows a spatial mixing of temperature classes. Consequently, the clear division into three groups cannot be continued. In addition, the general spread in this case is also significantly narrower than that of the average water

temperature, so the air temperature does not differ that much between the catchment areas. Yet, Figure B.5 illustrates that especially in the cold classified lakes, the air temperature is significantly higher compared to the water temperature, suggesting that particularly in these cases, the water temperature depends only to a limited extent on the air temperature. Other factors, such as snowmelt or exposure, could therefore have a stronger influence on the water temperature than the surrounding air temperature. In the case of warm classified lakes, an inverse shift can be observed: the air temperature is below the water temperature in the majority of lakes. Although the differences are smaller than in the cold classified lakes, especially in the case of Hohensee, Oberer Giglachsee, Unterer Giglachsee and Schwarzensee (i.e. lakes with  $\Delta > 1.22$  K, there is the possibility that other factors, like radiation or exposure, also have an influence on the water temperature.

It can therefore be stated that the water temperature cannot be solely explained by air temperature. Especially the cold classified lakes clearly stand out, but also a few warm classified lakes suggest that other factors influence the water temperature.

### 4.3 Approach III – Catchment energy input

#### Results

The following four Figures show the results of the Equations 3.3 and 3.4 each for the months JJA and the rest of the year. For more information, please consider Table A.4 on page 57 in Appendix A for more information.

Figure 4.6 visualizes the results of approach III regarding the mean energy input during the summer months JJA, with the x-axis representing the average yearly energy input of the catchment in  $\text{K mm m}^{-2}$  and the y-axis indicating the elevation of the respective lake in m a.s.l.. The distribution of the lakes shows no similarities to previous figures, the lakes are rather heterogeneously distributed, which means that the temperature classes cannot be distinguished from one another based on characteristic energy input limits. Generally it can not be said that the input decreases with increasing altitude. Lakes classified as warm are scattered over the whole range of the plot, with 4 of the 5 lakes with the greatest energy input being warm classified lakes. Although Oberer Schoenalmsee has a comparatively low average energy input of  $1,365 \text{ K mm m}^{-2}$  during the summer months, Unterer Klaftersee with  $1,667 \text{ K mm m}^{-2}$  has the highest entry of the dataset. The third highest value comes from a normally classified lake, the Gruensee with  $1,630 \text{ K mm m}^{-2}$ . While the other lakes classified as having a normal temperature can be found in all areas, Twenger Almsee receives the lowest average energy input during the summer with  $1,353 \text{ K mm m}^{-2}$ . Those classified as cold are located on an almost linear straight line in the center of the figure, with the Rauhenbergsee with  $1,449 \text{ K mm m}^{-2}$  as the lake with the lowest energy input. The Wildlochsee has the highest energy input of the group with  $1,574 \text{ K mm m}^{-2}$ .

In addition to Figure 4.6, Figure 4.7 shows the average yearly energy input of the

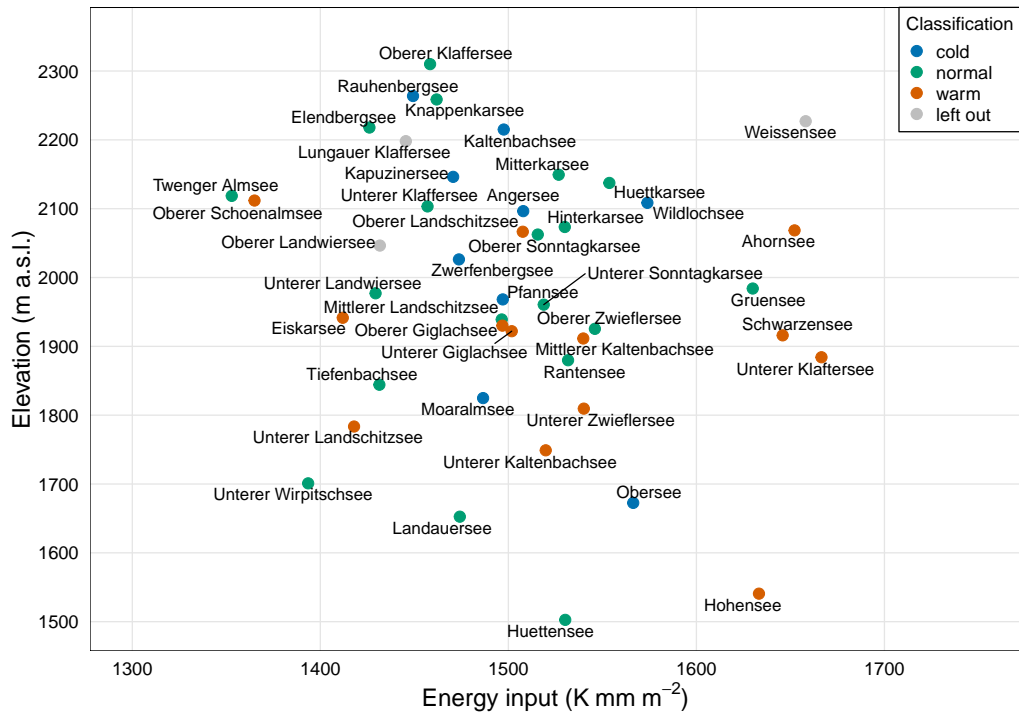


**Figure 4.6:** Average energy input during the summer months JJA, based on air temperature and precipitation lapse rates.

catchment areas during the remaining months of the year - September to May. Although the shape of the two graphs is similar, the energy input values for the other months are 700 to 800  $\text{K mm m}^{-2}$  lower than for the summer months. All but one lake classified as warm have an average energy input of over 700  $\text{K mm m}^{-2}$ . Similar to the JJA scenario, the Unterer Klaffersee with 906  $\text{K mm m}^{-2}$  has the highest energy input of the data set. With 659  $\text{K mm m}^{-2}$ , the Oberer Schoenalmsee is the warmest lake with the lowest energy input in this scenario; during the summer months, it even had the second lowest. As in the previous figure, the lakes classified as normal are distributed over the entire range of the x-axis, as the Twenger Almsee with 655  $\text{K mm m}^{-2}$  represents the lowest value of the entire dataset. Both lakes Unterer Wirpitschsee and Tiefenbachsee have a comparatively low average energy input of 671  $\text{K mm m}^{-2}$  and 683  $\text{K mm m}^{-2}$ , while again, Gruensee with 873  $\text{K mm m}^{-2}$  is the normally classified lake with the highest energy input. 6 of the 9 lakes classified as cold have an average energy input of more than 800  $\text{K mm m}^{-2}$  between September and May. The Wildlochsee with 892  $\text{K mm m}^{-2}$  has the highest, while the Rauhenbergsee with 772  $\text{K mm m}^{-2}$  has the lowest value of the group.

In contrast to the previous two figures, only the energy input that reaches the catchment areas on days with an average air temperature of less than 273.15 K is shown in the graphs that follow. Figure 4.8 shows the average yearly energy input during JJA and Figure 4.9 that of the remaining months.

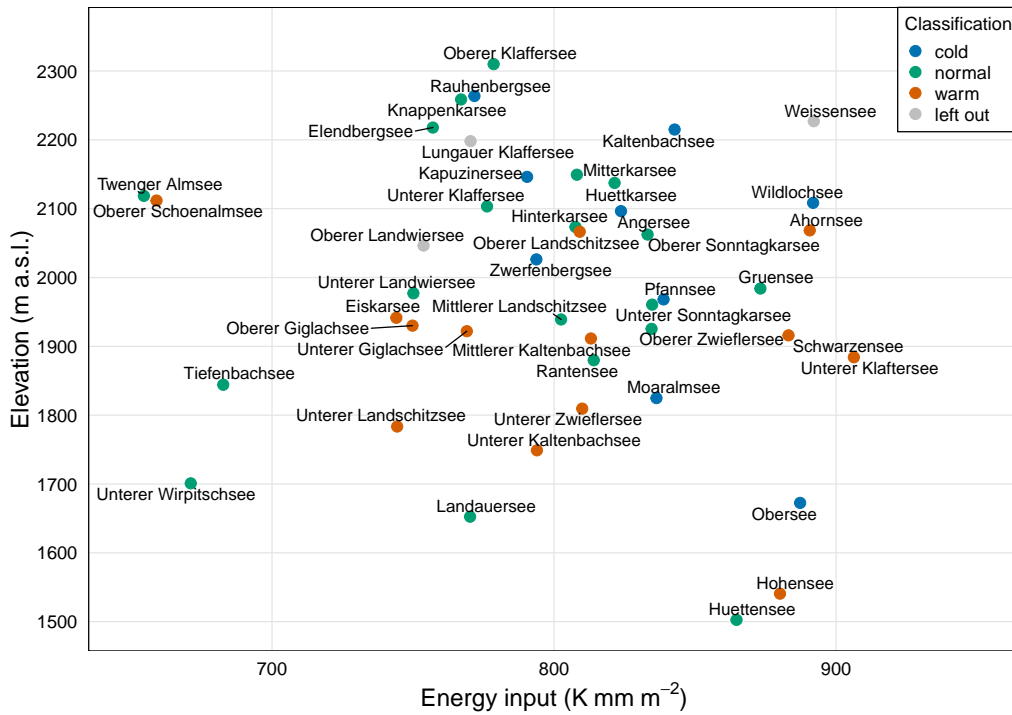


**Figure 4.7:** Average energy input during the months September to May, based on air temperature and precipitation lapse rates.

If one looks at this energy input during the summer months, it is striking that the values for most of the lakes are very low compared to the previously calculated average energy input. So the input of more than half of the lakes is below  $1,000 \text{ K mm m}^{-2}$ , whereas three cold, three normal and one warm classified lakes have values higher than  $1,500 \text{ K mm m}^{-2}$ . None of the cold classified lakes has a lower energy input than Moaralmsee with  $827 \text{ K mm m}^{-2}$ . Moreover, it is remarkable that all but two of the lakes classified as warm have an energy input of more than  $1,000 \text{ K mm m}^{-2}$ . Three of the warm classified lakes, Unterer Kaltenbachsee, Mittlerer Kaltenbachsee and Unterer Zwiefeldersee, have values below  $20 \text{ K mm m}^{-2}$ . The normal classified lakes are again distributed over the whole range of the x-axis, with the Elendbergsee with having the highest value of the dataset  $1,715 \text{ K mm m}^{-2}$ .

The energy input for the remaining months of the year in Figure 4.9 shows a similar shape. Here, the values are much higher and range between  $56,873 \text{ K mm m}^{-2}$  at Unterer Wirpitschsee (normal classified) and  $121,367 \text{ K mm m}^{-2}$  at Wildlochsee (cold classified). The warm classified lakes range from  $61,019 \text{ K mm m}^{-2}$  at Unterer Kaltenbachsee to  $103,172 \text{ K mm m}^{-2}$  at Ahornsee and show a rather low average energy inputs compared with the other groups. Cold classified lakes are more likely to be found on the right side of the diagram. All but the Moaralmsee with  $93,050 \text{ K mm m}^{-2}$  and two other lakes show values larger than  $100,000 \text{ K mm m}^{-2}$  whereas the Wildlochsee, as mentioned above, has the largest negative average energy input of the data set. No underlying trend can be observed for the lakes classified as normal. They rank from  $56,873$  (Unterer Wirpitschsee above) to  $112,806 \text{ K mm m}^{-2}$  at Oberer Sonntagkarsee.

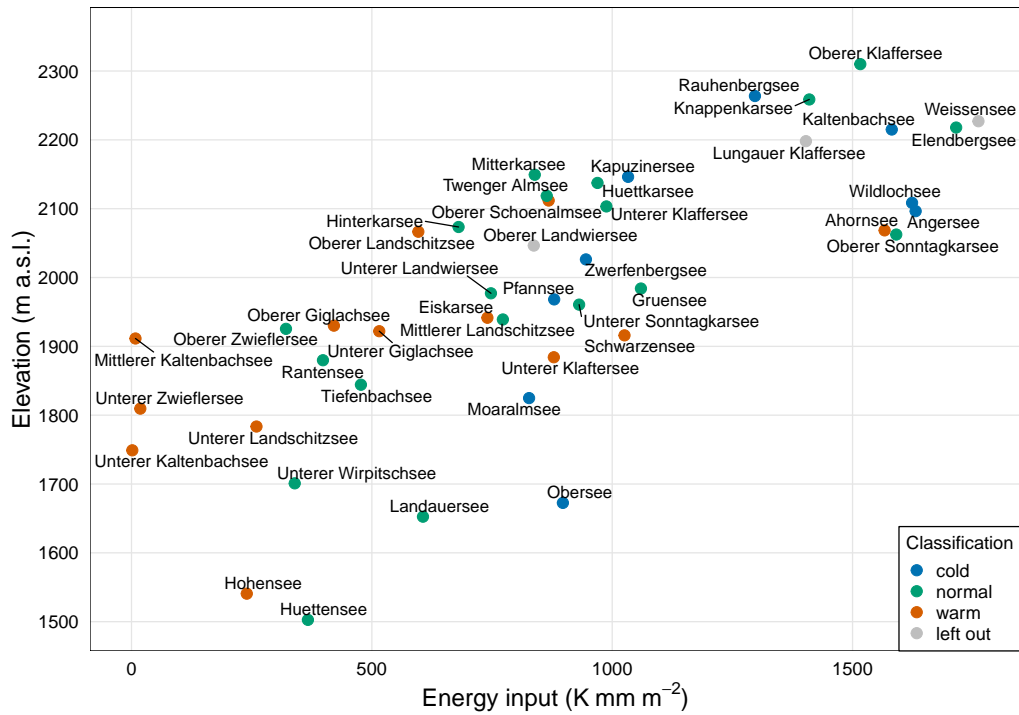


**Figure 4.8:** Average energy input for days with a negative air temperature during the summer months JJA, based on temperature and precipitation lapse rates.

## Discussion

In terms of the calculated energy inputs of the catchment areas, some generalisations may be deduced from this. Firstly, the warm classified lakes are in all cases more likely to be found on the right side of the diagrams, i.e. they receive on average more positive (or less negative) energy input, while the cold classified lakes are more likely to be on the left side of the diagrams, i.e. they receive on average more negative (or less positive) energy input. Equation 3.3 is used to calculate the total energy input, it is therefore not possible to determine in which ratio it is composed of a high temperatures or high precipitation. By contrast, Equation 3.4 is limited to the energy input on days with a negative mean air temperature in the catchment areas. Table A.5 in Appendix A on 58 presents for clarification purposes the mean monthly precipitation for all catchment areas calculated by means of SPARTACUS, as well as their mean monthly precipitation totals for the months JJA and September to May. The precipitation has been calculated by the same method that was already used to calculate the air temperature. The precipitation lapse rate for each catchment area was calculated by using corresponding SPARTACUS cells, which is then further used to calculate the catchments daily precipitation sums by taking the topography into account. The mean monthly precipitation sums for the two considered periods, summer versus the rest of the year, are shown in Table 4.1.

The standard deviation is comparatively high for both periods with regard to all temperature classes so that the mean monthly precipitation totals of the different classes do not differ significantly from each other. It would therefore be unreasonable to draw specific conclusions from the data set based on general energy input.

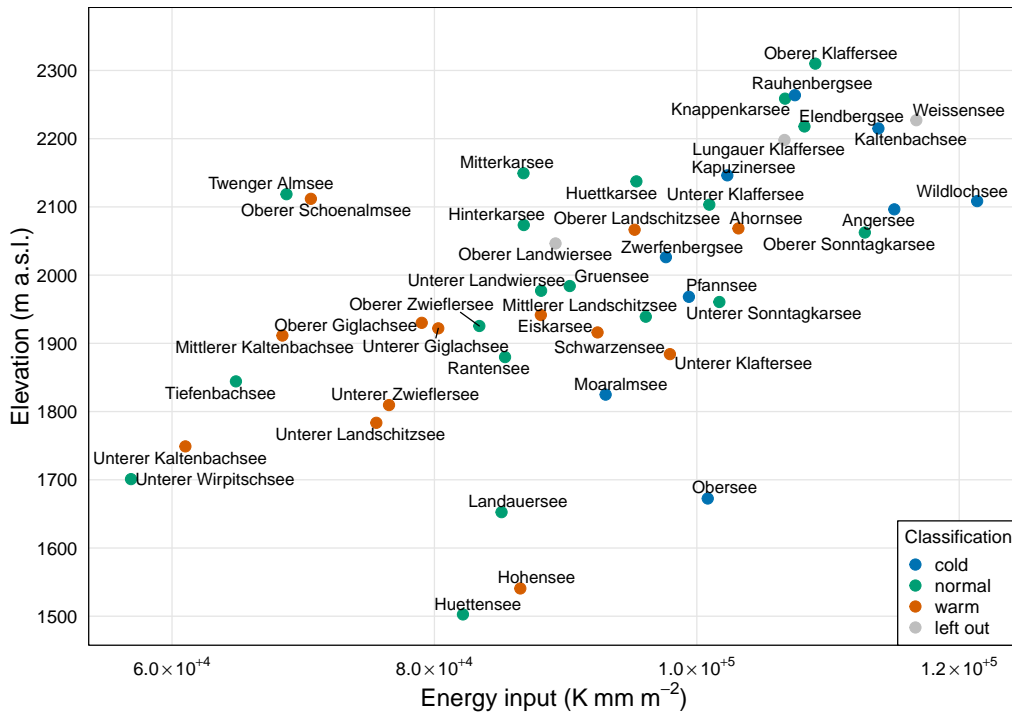


**Figure 4.9:** Average energy input for days with a negative air temperature during the months September to May, based on air temperature and precipitation lapse rates.

Temperature classification	JJA		September to May	
	Average monthly precipitation sum (mm)	Standard deviation	Average monthly precipitation sum (mm)	Standard deviation
Cold	138.6	5.0	92.7	4.6
Normal	136.0	9.7	87.2	6.8
Warm	142.1	13.7	89.1	8.0

**Table 4.1:** Average monthly precipitation sums and standard deviation for each temperature classification group for JJA and rest of the year.

For the summer months, arguably, the energy input is very low on average due to the rare occurrence of days with an average air temperature below 273.15 K. If it can be assumed, that precipitation occurring below 273.15 K falls as snow, there is consequently no or only negligible snowfall in the catchment areas during the summer months, as the values are rather small. The situation is different for the energy input on days with an average air temperature below 273.15 K during the rest of the year. At an energy input of about  $100,000 \text{ K mm m}^{-2}$ , the warm and cold classified lakes may be separated: Warm classified lakes thus have a lower average negative energy input than cold classified lakes and outside the summer months, more snow falls in the catchment areas of cold lakes than in those of warm lakes. This snow could therefore remain in the system as an energy-storage and then thaw by summer, entailing a colder water temperature during the months JJA. As shown in Figure 4.5, the air temperature during the summer months does not differ noteworthy between the catchment areas. In other words it has only a small impact on the water temperature of the lakes.

## 5. Conclusion and outlook

With regard to the three simplified hypotheses, there are clear indications that they should be rejected for the most part. Regarding the first hypothesis that the lakes have different water temperatures solely because of the topography of their catchment areas, not sufficient evidence can be found. In fact, the hypothesis applies to at least one of the graphically represented groups, group 1 (see Figure 4.1), but not to the other three. The topography of the catchment areas may therefore have an influence on the water temperature, but the different proportions of altitude zones alone cannot be held responsible for the substantial differences. Approach two, assuming a relationship between the lake water and air temperature lapse rate, cannot be confirmed either. Where similar studies (cf. McCombie (1959); Matuszek & Shuter (1996); Livingstone & Lotter (1998); Sharma et al. (2008)) show a correlation, the lapse rate of the air temperature shows a different distribution and average gradient compared to the water temperature. The calculated mean air temperature within the catchment areas does not show large deviations and therefore probably does not contribute much to the water temperatures of the lakes. For the third approach, by combining the air temperature and precipitation data from SPARTACUS, both the total energy input and the energy input for days with negative mean air temperature were modelled. Although the general energy input shows a tendency for warm lakes to be supplied with more energy in the summer than cold classified lakes, it leaves much room for interpretation, since it has not become clear whether the high input is due to the air temperature or precipitation. Concerning the negative energy input, it has been shown for both periods that warm classified catchments receive generally less input than cold classified ones. Especially during the months from September to May, a higher negative input can be observed for the cold classified lakes. These indications suggest that the influence of snowmelt might possibly be the biggest contributor to the fluctuation of water temperature between the lakes. In conclusion, however, this work cannot provide final proof of this.

### Outlook

Apart from the snowmelt, the different water temperature of the lakes during the summer months could also be influenced by other conditions. Further research towards the influence of meteorological input like radiation could provide more insight into the temperature anomalies, which is already subject to Matulla's work within the CLAIMES project. In addition to that, the morphological characteristics of the lakes could also have a major impact on the water temperature, as, for example, the water temperature of shallow lakes generally reacts faster to external influences than that of deep lakes.

For further research in this area, it would also be helpful if the measured data would be better archived. For example, the data on lake water temperature has been subject to

confusion, as it was not feasible to reproduce the results of Thompson et al. study. Also meta-data on the measured values, such as the installation depth and exact positioning in the lake is relevant for the analysis and furthermore nowadays easy to carry out using GPS. In addition to the already high-resolution (but compared to the size of some catchment areas rather coarse) meteorological data from SPARTACUS, local measurements would further enhance the database. Also the lapse rate of the air temperature calculated from the SPARTACUS cells ( $4.61 \text{ K km}^{-1}$ ) differs from the usually measured lapse in the Alps. The lapse rate of the previous study by Thompson et. al. was  $-6.25 \text{ K km}^{-1}$  and also values from the literature (Barry & Blanken, 2016) are rather in the range of about  $-6 \text{ K km}^{-1}$ . It is therefore possible that the used meteorological data might not be suitable for reconstructing such relatively small spatial structures. These deviations in air temperature lapse rate can potentially occur due to the topographic variability of the study area, I suggest, the accuracy of these spatially interpolated data should be critically assessed. In addition to the local air temperature, precipitation, lake water level and runoff, information on the snow pack could also be valuable. Combining the already existing data with the new data on water temperature collected by the on-going CLAIMES project, a more sound statement on the background of temperature anomalies of the investigated lakes should be soon possible.

# References

- Barry, R. G., & Blenkinsop, P. D. (2016). *Microclimate and local climate*. Cambridge University Press.
- Brondizio, E., Settele, J., Díaz, S., & Ngo, H. (2019). Global assessment report on biodiversity and ecosystem services of the intergovernmental science-policy platform on biodiversity and ecosystem services. *IPBES Secretariat*.
- Edinger, J. E., Duttweiler, D. W., & Geyer, J. C. (1968). The response of water temperatures to meteorological conditions. *Water Resources Research*, 4(5), 1137–1143.
- Fontana, V., Kurmayer, R., Schirpke, U., Ohndorf, M., & Matulla, C. (2019). *CLimate response of Alpine lakes Project*. Retrieved 10.09.2019, from <https://www.uibk.ac.at/projects/claimes/>
- Geological Survey of Austria. (2005). *Geologische Karte von Salzburg (1:200,000)*. Author. (Pestal, G. and Hejl, E. and others)
- Geo Scientific Inc., A. R. R. (2001). *Dedicated water level data loggers*. Retrieved 13.11.2019, from <http://www.geoscientific.com/dataloggers/Specifications/MiniLog.html>
- Hedderich, J., & Sachs, L. (2018). *Angewandte Statistik*. Springer.
- Hiebl, J., & Frei, C. (2016). Daily temperature grids for Austria since 1961 – concept, creation and applicability. *Theoretical and applied climatology*, 124(1-2), 161–178.
- Hiebl, J., & Frei, C. (2018). Daily precipitation grids for Austria since 1961 – development and evaluation of a spatial dataset for hydroclimatic monitoring and modelling. *Theoretical and applied climatology*, 132(1-2), 327–345.
- Hutchinson, G. E. (1975). *A treatise on limnology 1, Geography, physics, and chemistry, Part 1 Geography and physics of lakes*. Wiley.
- Kettle, H., Thompson, R., Anderson, N. J., & Livingstone, D. M. (2004). Empirical modeling of summer lake surface temperatures in southwest Greenland. *Limnology and Oceanography*, 49(1), 271–282.
- Kum, G. (1999). *Gis-Bearbeitung 45 Seen* (Tech. Rep.). Österreichische Akademie der Wissenschaften, Institut für Limnologie, 5310 Mondsee.
- Lane, R. K. (2019). *Lake*. Retrieved 15.01.2020, from <https://www.britannica.com/science/lake>

- Lewis Jr., W. M. (1983). A revised classification of lakes based on mixing. *Canadian Journal of Fisheries and Aquatic Sciences*, 40(10), 1779–1787.
- Livingstone, D. M., & Imboden, D. M. (1989). Annual heat balance and equilibrium temperature of Lake Aegeri, Switzerland. *Aquatic Sciences*, 51(4), 351–369.
- Livingstone, D. M., & Lotter, A. F. (1998). The relationship between air and water temperatures in lakes of the Swiss Plateau. *Journal of Paleolimnology*, 19(2), 181–198.
- Livingstone, D. M., Lotter, A. F., & Walkery, I. R. (1999). The decrease in summer surface water temperature with altitude in Swiss Alpine lakes: a comparison with air temperature lapse rates. *Arctic, Antarctic, and Alpine Research*, 31(4), 341–352.
- Maniak, U. (2016). *Einführung Hydrologie und Wasserwirtschaft*. Springer.
- Marti, D. E., & Imboden, D. M. (1986). Thermische Energieflüsse an der Wasseroberfläche: Beispiel Sempachersee. *Swiss journal of hydrology*, 48(2), 196–229.
- Matuszek, J. E., & Shuter, B. J. (1996). An empirical method for the prediction of daily water temperatures in the littoral zone of temperate lakes. *Transactions of the American Fisheries Society*, 125(4), 622–627.
- McCombie, A. (1959). Some relations between air temperatures and the surface water temperatures of lakes. *Limnology and Oceanography*, 4(3), 252–258.
- Messer, M., & Schneider, G. (2019). *Statistik: Theorie und Praxis im Dialog*. Springer-Verlag.
- O'Sullivan, P., Reynolds, C., et al. (2004). *The lakes handbook 1 Limnology and limnetic ecology*. Blackwell Publishing.
- O'Sullivan, P., Reynolds, C., et al. (2005). *The lakes handbook 2 Lake restoration and rehabilitation*. Blackwell Publ.
- Piccolroaz, S., Toffolon, M., & Majone, B. (2013). A simple lumped model to convert air temperature into surface water temperature in lakes. *Hydrology and Earth System Sciences*, 17(8), 3323–3338.
- Schmidt, R., Kamenik, C., Kaiblinger, C., & Hetzel, M. (2004). Tracking Holocene environmental changes in an alpine lake sediment core: application of regional diatom calibration, geochemistry, and pollen. *Journal of Paleolimnology*, 32(2), 177–196.
- Schmidt, R., Kamenik, C., Lange-Bertalot, H., & Klee, R. (2004). *Fragilaria* and *Staurosira* (Bacillariophyceae) from sediment surfaces of 40 lakes in the Austrian Alps in relation to environmental variables, and their potential for palaeoclimatology. *Journal of Limnology*, 63, 171–189.

- Sharma, S., Walker, S. C., & Jackson, D. A. (2008). Empirical modelling of lake water-temperature relationships: a comparison of approaches. *Freshwater biology*, 53(5), 897–911.
- Šporka, F., Livingstone, D., Stuchlík, E., Turek, J., & Galas, J. (2006). Water temperatures and ice cover in lakes of the Tatra Mountains. *Biologia*, 61(18), S77–S90.
- Thompson, R., Kamenik, C., & Schmidt, R. (2005). Ultra-sensitive Alpine lakes and climate change. *Journal of Limnology*, 64(2), 139–152.
- Weckström, K., Weckström, J., Huber, K., Kamenik, C., Schmidt, R., Salvenmoser, W., ... Kurmayer, R. (2016). Impacts of climate warming on Alpine lake biota over the past decade. *Arctic, Antarctic, and Alpine Research*, 48(2), 361–376.
- Wetzel, R. G. (2001). *Limnology: lake and river ecosystems*. Elsevier.

# List of Tables

2.1	General information about the lakes: as coordinates (after MGI / Austria GK M31), elevation, maximum depth, water surface. . . . .	16
3.1	Some statistics about the lakes with missing data. . . . .	21
4.1	Average monthly precipitation sums and standard deviation for each temperature classification group for JJA and rest of the year. . . . .	43
A.1	Some statistics about the lake water temperature dataset. . . . .	53
A.2	Landcover information from CORINE about the catchments of the dataset. First column of each category shows area in ha and second column in percentage of whole watershed. . . . .	55
A.3	Comparison of average summer water temperature of previous paper and results by calculation with databasis for JJA. Also the average summer air temperature of each catchment and its temperature class are displayed.	56
A.4	Results of the Equations 3.3 and 3.4 of the third approach for the months JJA and the remaining year respectively. . . . .	57
A.5	Average precipitation sums for the months JJA and the rest of the year, as well as average monthly precipitation sums for all catchments based on spatially interpolated data. . . . .	58

# List of Figures

1.1	Main heat fluxes interacting with the water surface, taken from Piccolroaz et al. (2013) . . . . .	6
2.1	Location of the study area and the lakes, taken from Thompson et al. (2005) . . . . .	14
2.2	Predominant catchments of the research area (red box) as of . . . . .	16
2.3	Land cover according to CLC (as of 2018). . . . .	17
2.4	Geology of the study area (as of Geological Survey of Austria (2005)). . . . .	18
3.1	DEM of the research area with lake/catchment polygons and used SPARTACUS cells . . . . .	22
3.2	Close-up of 50 m elevation steps within each catchment and used SPARTACUS cells for Knappenkarsee, Landauersee, Oberer Giglachsee and Unterer Giglachsee (marked red). . . . .	23
3.3	Classification based on paper by Thompson et al. (2005), with the diagonal lines displaying the air-temperature lapse rate. . . . .	25
3.4	Classification based on received data, with the diagonal lines displaying the air-temperature lapse rate calculated with SPARTACUS data. . . . .	26
3.5	Limits and numbering of lake groups . . . . .	27
4.1	Group 1: Elevation density distribution of Angersee, Wildlochsee, Twenger Almsee, Unterer Klaffersee and Oberer Schoenalmsee . . . . .	31
4.2	Group 2: Elevation density distribution of Zwerfenbergsee, Oberer Sonntagkarsee, Ahornsee and Oberer Landschitzsee . . . . .	32
4.3	Group 3: Elevation density distribution of Pfannsee, Mittlerer Landschitzsee, Unterer Landwiersee, Unterer Sonntagkarsee, Eiskarsee and Oberer Giglachsee . . . . .	34
4.4	Group 4: Elevation density distribution of Moaralmsee, Tiefenbachsee and Unterer Zwiefldersee. . . . .	36
4.5	Average air temperature of each catchment for the summer months June, July and August compared to lake elevation. The diagonal lines displaying the air-temperature lapse rate calculated with SPARTACUS data. . . . .	38
4.6	Average energy input during the summer months JJA, based on air temperature and precipitation lapse rates. . . . .	40
4.7	Average energy input during the months September to May, based on air temperature and precipitation lapse rates. . . . .	41

4.8	Average energy input for days with a negative air temperature during the summer months JJA, based on temperature and precipitation lapse rates.	42
4.9	Average energy input for days with a negative air temperature during the months September to May, based on air temperature and precipitation lapse rates. . . . .	43
B.1	Comparison of the summer water temperatures reported by the initial study and the mean values for the month of June calculated with the obtained raw data. . . . .	59
B.2	Comparison of the summer water temperatures reported by the initial study and the mean values for the month of July calculated with the obtained raw data. . . . .	60
B.3	Comparison of the summer water temperatures reported by the initial study and the mean values for the month of August calculated with the obtained raw data. . . . .	60
B.4	Comparison of the plotted summer water temperature values of the initial study and the data provided for this master thesis. . . . .	61
B.5	Approach 2: Shifting of values from mean summer water temperature of the lake to mean summer air temperature of the catchment. . . . .	61

# Appendices

# A. Tables

Id	Name	Date		Total	Days		# of used thermistor
		Start	End		Missing abs.	Missing %	
1	Ahornsee	28.08.98	04.08.03	1802	0	0.0	2
2	Angersee	24.08.98	08.08.03	1810	0	0.0	1
3	Eiskarsee	31.08.98	31.08.03	1826	0	0.0	1
4	Elendbergsee	31.08.98	31.08.03	1826	0	0.0	1
5	Gruensee	19.07.98	05.08.03	1843	0	0.0	1
6	Hinterkarsee	07.09.98	27.07.03	1784	0	0.0	1
7	Hohensee	20.07.98	05.08.03	1842	1	0.1	1
8	Huettensee	02.08.98	24.07.03	1817	2	0.1	1
9	Huettkarsee	30.08.98	26.07.03	1791	0	0.0	1
10	Kaltenbachsee	03.08.98	17.08.03	1840	0	0.0	1
11	Kapuzinersee	12.09.98	09.08.03	1792	0	0.0	2
12	Knappenkarsee	07.09.98	02.08.03	1790	0	0.0	1
13	Landauersee	17.07.98	20.07.03	1829	1	0.1	1
14	Lungauer Klaffersee	24.08.98	23.09.99	395	0	0.0	1
15	Mitterkarsee	07.09.98	31.07.01	1058	0	0.0	1
16	Mittlerer Kaltenbachsee	12.07.98	22.07.03	1836	0	0.0	1
17	Mittlerer Landschitzsee	21.08.98	08.08.03	1813	0	0.0	1
18	Moaralmsee	24.07.98	19.07.03	1821	0	0.0	1
19	Oberer Giglachsee	05.09.98	10.08.03	1800	0	0.0	1
20	Oberer Klaffersee	13.09.98	08.08.03	1790	0	0.0	2
21	Oberer Landschitzsee	21.08.98	08.08.03	1813	0	0.0	1
22	Oberer Landwiersee	09.09.98	07.09.99	363	0	0.0	1
23	Oberer Schoenalmsee	27.07.98	02.08.03	1832	0	0.0	1
24	Oberer Sonntagkarsee	15.09.98	10.08.03	1790	0	0.0	1
25	Oberer Zwiefeldersee	13.07.98	23.07.03	1836	0	0.0	1
26	Obersee	02.08.98	24.07.03	1817	0	0.0	2
27	Pfannsee	03.08.98	17.08.03	1840	0	0.0	1
28	Rantensee	07.09.98	27.07.03	1784	0	0.0	1
29	Rauhenbergsee	14.09.98	08.08.03	1789	0	0.0	1
30	Schwarzensee	19.07.98	05.08.03	1843	0	0.0	1
31	Tiefenbachsee	26.07.98	01.08.03	1832	0	0.0	1
32	Twenger Almsee	27.07.98	02.08.03	1832	0	0.0	1
33	Unterer Giglachsee	05.09.98	10.08.03	1800	411	22.8	1
34	Unterer Kaltenbachsee	12.07.98	22.07.03	1836	0	0.0	2
35	Unterer Klaffersee	14.09.98	08.08.03	1789	0	0.0	2
36	Unterer Klaftersee	27.08.98	04.08.03	1803	0	0.0	1
37	Unterer Landschitzsee	20.08.98	19.08.03	1825	0	0.0	2
38	Unterer Landwiersee	09.09.98	22.08.03	1808	0	0.0	2
39	Unterer Sonntagkarsee	15.09.98	10.08.03	1790	0	0.0	1
40	Unterer Wirpitschsee	26.07.98	02.08.03	1833	0	0.0	2
41	Unterer Zwiefeldersee	13.07.98	23.07.03	1836	0	0.0	1
42	Weissensee	28.08.98	31.08.99	368	0	0.0	2
43	Wildlochsee	11.09.98	10.08.03	1794	448	25.0	2
44	Zwerfenbergsee	23.08.98	09.08.03	1812	0	0.0	1

**Table A.1:** Some statistics about the lake water temperature dataset.

No	Lake	Landcover											
		Area					Landcover						
		Total	Water bodies	Coniferous forest	Natural grassland	Moors and heathland	Bare rocks	Sparsely vegetated areas					
1	Ahornsee	67.4	2.5	3.7	0.0	0.0	46.7	69.3	0.0	0.0	0.0	18.2	27.0
2	Angersee	98.0	3.1	3.2	0.0	0.0	14.6	14.9	0.0	0.0	0.0	80.2	81.9
3	Eiskarsee	65.5	2.7	4.1	0.0	0.0	0.2	0.3	0.0	0.0	0.0	62.6	95.6
4	Elendbergsee	52.9	3.3	6.2	0.0	0.0	0.0	0.0	0.0	0.0	0.0	49.6	93.8
5	Gruensee	92.2	3.0	3.2	0.0	0.0	34.2	37.1	1.0	1.0	0.0	54.1	58.7
6	Hinterkarsee	47.9	1.8	3.8	0.0	0.0	24.4	51.0	0.0	0.0	0.0	21.6	45.2
7	Hohensee	282.8	4.6	1.6	7.4	2.6	131.8	46.6	122.5	43.3	0.0	16.5	5.8
8	Huettensee	144.3	4.7	3.2	0.0	0.0	102.7	71.2	18.6	12.9	0.0	18.3	12.7
9	Huettkarsee	35.4	0.9	2.6	0.0	0.0	2.2	6.3	0.0	0.0	0.0	32.2	91.0
10	Kaltenbachsee	16.0	0.6	3.8	0.0	0.0	0.0	0.0	0.0	0.0	0.0	15.4	96.2
11	Kapuzinersee	31.5	2.2	6.8	0.0	0.0	5.8	18.4	0.0	0.0	0.0	23.6	74.8
12	Knappenkarsee	21.1	1.8	8.7	0.0	0.0	0.0	0.0	0.0	0.0	0.0	19.2	91.3
13	Landauersee	631.4	3.6	0.6	23.1	3.7	234.3	37.1	64.9	10.3	0.0	305.5	48.4
14	Lungauer Klaffersee	78.3	4.4	5.6	0.0	0.0	0.0	0.0	0.0	0.0	0.0	74.0	94.4
15	Mitterkarsee	36.5	2.7	7.3	0.0	0.0	6.8	18.6	0.0	0.0	0.0	27.1	74.1
16	Mittlerer Kaltenbachsee	29.3	2.3	7.7	0.0	0.0	25.0	85.4	0.0	0.0	0.0	2.0	6.9
17	Mittlerer Landschitzsee	282.3	6.0	2.1	0.0	0.0	71.0	25.1	0.0	0.0	0.0	205.3	72.7
18	Moaralmsee	109.5	2.0	1.9	0.0	0.0	18.6	17.0	0.0	0.0	0.0	88.8	81.1
19	Oberer Giglachsee	95.4	3.4	3.6	0.0	0.0	55.7	58.3	0.0	0.0	0.6	35.7	37.4
20	Oberer Klaffersee	60.9	5.1	8.4	0.0	0.0	0.0	0.0	0.0	0.0	0.0	55.8	91.6
21	Oberer Landschitzsee	74.7	8.7	11.7	0.0	0.0	12.0	16.1	0.0	0.0	0.0	54.0	72.3
22	Oberer Landwiersee	62.5	4.0	6.4	0.0	0.0	13.4	21.4	0.0	0.0	0.0	45.1	72.2
23	Oberer Schoenalmsee	31.6	5.1	16.1	0.0	0.0	24.1	76.3	0.0	0.0	0.0	2.4	7.6
24	Oberer Sonntagkarsee	107.1	6.5	6.1	0.0	0.0	0.5	0.5	0.0	0.0	0.0	100.1	93.4
25	Oberer Zwieflersee	119.2	3.0	2.5	0.0	0.0	76.7	64.3	1.0	0.9	0.0	38.4	32.2
26	Obersee	301.3	7.0	2.3	0.0	0.0	106.5	35.3	0.3	0.1	65.8	21.8	121.7

No	Lake	Area										Landcover									
		Total	Water bodies	Coniferous forest	Natural grassland	Moors and heathland	Bare rocks	Sparsely vegetated areas	Total	Water bodies	Coniferous forest	Natural grassland	Moors and heathland	Bare rocks	Sparsely vegetated areas						
27	Pfannsee	121.7	1.5	1.2	0.0	0.0	13.0	10.7	0.0	0.0	26.6	21.8	80.7	66.3							
28	Rantensee	127.0	2.2	1.7	0.0	0.0	47.9	37.7	0.0	0.0	0.0	0.0	76.9	60.6							
29	Rauhenbergsee	44.5	2.7	6.1	0.0	0.0	0.0	0.0	0.0	0.0	0.0	0.0	41.8	93.9							
30	Schwarzensee	128.2	3.7	2.9	0.0	0.0	79.6	62.1	8.3	6.5	0.0	0.0	36.6	28.5							
31	Tiefenbachsee	136.6	3.3	2.4	0.0	0.0	46.9	34.4	0.0	0.0	0.0	0.0	86.3	63.2							
32	Twenger Almsee	13.2	2.9	21.9	0.0	0.0	8.5	64.1	0.0	0.0	0.0	0.0	1.9	14.0							
33	Unterer Giglachsee	178.9	16.2	9.0	0.0	0.0	96.4	53.9	0.0	0.0	0.0	0.0	66.4	37.1							
34	Unterer Kaltenbachsee	127.9	5.6	4.4	0.0	0.0	121.6	95.1	0.0	0.0	0.0	0.0	0.7	0.6							
35	Unterer Klaffersee	36.1	3.7	10.3	0.0	0.0	5.1	14.2	0.0	0.0	0.0	0.0	27.3	75.6							
36	Unterer Klaftersee	96.6	1.6	1.7	0.0	0.0	77.4	80.2	0.0	0.0	0.0	0.0	17.5	18.1							
37	Unterer Landschitzsee	198.2	11.3	5.7	31.8	16.0	106.3	53.6	0.2	0.1	0.0	0.0	48.6	24.5							
38	Unterer Landwiersee	65.6	1.5	2.3	0.0	0.0	23.3	35.5	0.0	0.0	0.0	0.0	40.8	62.2							
39	Unterer Sonntagskarsee	106.2	4.8	4.5	0.0	0.0	19.1	18.0	0.0	0.0	0.0	0.0	82.4	77.5							
40	Unterer Wirpitschsee	126.8	2.7	2.1	0.5	0.4	61.3	48.4	13.6	10.8	0.0	0.0	48.7	38.4							
41	Unterer Zwieflersee	110.9	4.2	3.8	0.0	0.0	67.8	61.2	38.9	35.1	0.0	0.0	0.0	0.0							
42	Weissensee	57.3	6.3	11.0	0.0	0.0	4.3	7.5	0.0	0.0	0.0	0.0	46.7	81.5							
43	Wildlochsee	85.5	1.3	1.6	0.0	0.0	0.0	0.0	0.0	0.0	25.3	29.6	58.8	68.8							
44	Zwerfenbergsee	176.9	10.8	6.1	0.0	0.0	47.4	26.8	0.0	0.0	0.0	0.0	118.7	67.1							

**Table A.2:** Landcover information from CORINE about the catchments of the dataset. First column of each category shows area in ha and second column in percentage of whole watershed.

Id	Lake	Average summer water temperature (K)			Average summer air temperature (K)		Temperature class	
		Paper	Thesis	$\Delta$	Thesis	$\Delta$	Paper	Thesis
1	Ahornsee	282.9	282.9	0.0	282.6	-0.3	warm	warm
2	Angersee	281.2	279.9	-1.2	281.3	1.4	normal	cold
3	Eiskarsee	283.6	283.7	0.1	282.7	-1.0	normal	warm
4	Elendbergsee	281.4	280.5	-0.9	281.1	0.6	normal	normal
5	Gruensee	281.5	282.0	0.5	283.4	1.5	cool	normal
6	Hinterkarsee	282.9	282.6	-0.2	283.3	0.6	warm	normal
7	Hohensee	284.0	285.4	1.4	283.8	-1.6	unusually cold	warm
8	Huettensee	283.5	283.8	0.4	284.8	1.0	unusually cold	normal
9	Huettkarsee	280.9	280.6	-0.3	282.6	2.1	normal	normal
10	Kaltenbachsee	280.2	278.6	-1.6	282.0	3.4	cool	cold
11	Kapuzinersee	280.5	278.9	-1.5	282.0	3.1	cool	cold
12	Knappenkarsee	281.7	280.2	-1.4	281.4	1.1	warm	normal
13	Landauersee	283.1	283.9	0.8	283.4	-0.4	unusually cold	normal
14	Lungauer Klaffersee	281.4	280.7	-0.7	281.4	0.7	normal	left out
15	Mitterkarsee	282.5	282.0	-0.4	283.2	1.2	warm	normal
16	Mittlerer Kaltenbachsee	284.3	284.7	0.5	284.8	0.1	normal	warm
17	Mittlerer Landschitzsee	282.6	282.4	-0.2	282.3	0.0	normal	normal
18	Moaralmsee	280.5	280.2	-0.3	283.5	3.3	unusually cold	cold
19	Oberer Giglachsee	284.4	285.0	0.6	283.5	-1.5	warm	warm
20	Oberer Klaffersee	281.1	279.9	-1.2	281.2	1.3	normal	normal
21	Oberer Landschitzsee	283.8	283.6	-0.2	282.5	-1.1	hot	warm
22	Oberer Landwiersee	281.7	279.2	-2.5	282.4	3.2	normal	left out
23	Oberer Schoenalmsee	284.0	282.9	-1.0	282.5	-0.4	hot	warm
24	Oberer Sonntagkarsee	281.7	281.2	-0.5	281.6	0.5	normal	normal
25	Oberer Zwieflersee	282.6	282.5	-0.1	283.9	1.4	normal	normal
26	Obersee	282.7	282.4	-0.3	283.3	0.9	unusually cold	cold
27	Pfannsee	280.7	280.6	-0.1	283.1	2.5	unusually cold	cold
28	Rantensee	282.9	283.2	0.3	283.7	0.5	normal	normal
29	Rauhenbergsee	281.0	279.8	-1.1	281.3	1.5	normal	cold
30	Schwarzensee	283.4	284.4	1.0	283.2	-1.2	normal	warm
31	Tiefenbachsee	283.4	283.5	0.2	283.3	-0.2	normal	normal
32	Twenger Almsee	283.2	282.5	-0.7	282.6	0.2	hot	normal
33	Unterer Giglachsee	283.9	285.2	1.3	283.7	-1.5	normal	warm
34	Unterer Kaltenbachsee	283.9	285.3	1.4	285.5	0.2	normal	warm
35	Unterer Klaffersee	282.2	280.8	-1.4	282.0	1.3	normal	normal
36	Unterer Klaftersee	283.3	283.8	0.5	283.2	-0.6	normal	warm
37	Unterer Landschitzsee	284.4	284.5	0.1	283.8	-0.8	normal	warm
38	Unterer Landwiersee	282.1	282.1	0.0	282.6	0.5	normal	normal
39	Unterer Sonntagkarsee	282.4	281.9	-0.4	282.6	0.7	normal	normal
40	Unterer Wirpitschsee	283.3	283.5	0.2	284.0	0.5	cool	normal
41	Unterer Zwieflersee	283.9	284.8	0.9	284.2	-0.7	normal	warm
42	Weissensee	282.0	279.9	-2.0	281.6	1.7	warm	left out
43	Wildlochsee	281.3	279.5	-1.8	281.8	2.3	normal	cold
44	Zwerfenbergsee	281.9	280.6	-1.3	282.4	1.8	normal	cold

**Table A.3:** Comparison of average summer water temperature of previous paper and results by calculation with databasis for JJA. Also the average summer air temperature of each catchment and its temperature class are displayed.

Id	Lake	Average energy input (K mm m <sup>2</sup> )		Average energy input for air temp. <273.15 K (K mm m <sup>2</sup> )	
		JJA	Rest of the year	JJA	Rest of the year
1	Ahornsee	1,652.2	890.7	1,566.7	103,172.3
2	Angersee	1,507.9	823.7	1,631.2	115,052.7
3	Eiskarsee	1,411.9	744.1	740.4	88,112.4
4	Elendbergsee	1,426.1	757.0	1,715.5	108,205.0
5	Gruensee	1,630.0	873.2	1,059.8	90,313.4
6	Hinterkarsee	1,530.0	807.6	680.4	86,811.0
7	Hohensee	1,633.3	880.1	239.8	86,547.1
8	Huettensee	1,530.2	864.7	367.0	82,174.3
9	Huettkarsee	1,553.7	821.4	969.4	95,395.6
10	Kaltenbachsee	1,497.5	842.7	1,581.6	113,842.3
11	Kapuzinersee	1,470.6	790.4	1,033.0	102,325.0
12	Knappenkarsee	1,461.8	767.0	1,410.0	106,725.2
13	Landauersee	1,474.2	770.2	606.4	85,116.0
14	Lungauer Klaffersee	1,445.5	770.4	1,403.0	106,682.3
15	Mitterkarsee	1,526.8	808.1	838.9	86,789.6
16	Mittlerer Kaltenbachsee	1,539.8	813.1	8.3	68,413.4
17	Mittlerer Landschitzsee	1,496.5	802.5	772.6	96,112.3
18	Moaralmsee	1,486.6	836.3	827.1	93,049.8
19	Oberer Giglachsee	1,496.8	749.8	421.0	79,033.7
20	Oberer Klaffersee	1,458.4	778.6	1,516.1	109,032.2
21	Oberer Landschitzsee	1,507.7	809.1	596.7	95,259.5
22	Oberer Landwiersee	1,431.7	753.7	836.9	89,231.5
23	Oberer Schoenalmsee	1,365.0	659.0	867.8	70,584.5
24	Oberer Sonntagkarsee	1,515.6	833.2	1,590.9	112,806.3
25	Oberer Zwiefelersee	1,546.0	834.6	321.4	83,423.7
26	Obersee	1,566.4	887.2	897.4	100,832.7
27	Pfannsee	1,497.0	838.8	879.3	99,396.7
28	Rantensee	1,531.7	814.1	398.3	85,382.6
29	Rauhenbergsee	1,449.3	771.8	1,296.9	107,476.0
30	Schwarzensee	1,645.9	883.1	1,025.6	92,434.6
31	Tiefenbachsee	1,431.4	682.7	477.3	64,871.5
32	Twenger Almsee	1,352.9	654.6	863.9	68,723.6
33	Unterer Giglachsee	1,501.8	769.1	515.4	80,293.6
34	Unterer Kaltenbachsee	1,519.9	793.9	1.7	61,018.6
35	Unterer Klaffersee	1,457.0	776.2	987.9	100,952.3
36	Unterer Klaftersee	1,666.5	906.3	878.6	97,949.5
37	Unterer Landschitzsee	1,417.9		260.0	75,573.2
38	Unterer Landwiersee	1,429.4	750.1	747.8	88,131.4
39	Unterer Sonntagkarsee	1,518.8	834.8	931.2	101,718.8
40	Unterer Wirpitschsee	1,393.5	671.2	339.6	56,873.4
41	Unterer Zwiefelersee	1,540.1	810.0	18.3	76,539.1
42	Weissensee	1658.1	892.1	1,761.9	116,731.0
43	Wildlochsee	1573.9	891.8	1,623.8	121,366.9
44	Zwerfenbergsee	1,473.7	793.7	945.4	97,644.8

**Table A.4:** Results of the Equations 3.3 and 3.4 of the third approach for the months JJA and the remaining year respectively.

Id	Lake	JJA	S-M	J	F	M	A	M	J	J	A	S	O	N	D
1	Ahornsee	158.9	99.1	53.2	85.5	103.4	98.4	134.2	158.6	183.9	183.1	152.4	104.5	85.3	74.8
2	Angersee	138.6	92.2	63.8	83.1	98.9	83.0	110.4	143.7	161.7	175.9	131.3	101.3	81.2	76.4
3	Eiskarsee	126.6	82.8	55.5	69.6	94.9	74.9	102.3	128.6	148.9	170.3	118.3	84.8	79.3	66.1
4	Elendbergsee	128.7	84.7	57.0	72.4	98.2	77.3	104.1	131.3	150.9	172.7	118.9	86.5	80.6	67.6
5	Gruensee	155.8	96.8	52.1	82.6	100.9	95.1	132.5	153.9	181.1	181.5	147.7	103.5	84.8	72.6
6	Hinterkarsee	143.1	89.7	50.5	77.1	104.0	83.9	131.8	130.2	167.3	185.1	119.2	92.8	86.7	61.1
7	Hohensee	156.2	97.5	51.6	81.4	102.4	95.0	135.6	150.7	182.4	183.2	146.3	105.0	88.3	71.9
8	Huettensee	141.5	95.6	66.4	91.2	107.5	82.5	111.6	150.0	162.7	170.9	139.9	97.1	80.6	84.1
9	Huettkarsee	145.9	91.4	51.1	78.7	105.8	85.7	133.7	133.5	170.4	187.4	122.2	94.9	87.5	62.9
10	Kaltenbachsee	139.1	94.2	67.1	92.6	107.8	82.1	109.2	148.0	160.1	170.1	134.3	93.6	78.3	82.3
11	Kapuzinersee	134.3	88.2	60.7	78.7	94.9	78.5	106.6	138.4	157.8	171.9	126.9	96.4	78.6	72.6
12	Knappenkarsee	130.7	85.8	57.2	71.7	101.4	79.4	105.0	133.9	153.1	178.7	121.9	84.7	82.5	68.0
13	Landauersee	131.4	85.6	59.5	73.7	98.7	78.2	102.0	137.0	155.0	174.8	123.2	86.8	78.5	69.3
14	Lungauer Klaffersee	131.6	86.2	58.5	75.3	94.1	77.8	105.9	134.4	154.6	171.9	123.3	92.9	78.6	69.1
15	Mitterkarsee	143.6	89.7	50.5	76.3	103.3	83.6	130.6	132.3	168.0	181.8	122.3	93.5	85.9	61.7
16	Mittlerer Kaltenbachsee	146.1	89.7	46.6	71.8	91.7	89.6	127.6	140.9	169.8	174.3	134.7	99.9	82.2	63.6
17	Mittlerer Landschitzsee	137.1	89.4	52.3	72.8	111.0	84.5	128.2	122.9	160.2	189.5	114.7	87.8	93.0	60.2
18	Moaralmsee	137.5	92.9	66.2	90.1	106.1	80.7	107.9	146.0	158.5	167.5	133.1	92.9	77.9	81.6
19	Oberer Giglachsee	132.2	83.2	55.4	67.4	96.0	76.1	103.5	136.2	156.9	180.4	122.1	82.9	79.7	65.8
20	Oberer Klaffersee	133.1	87.1	59.4	77.1	94.7	78.5	106.5	136.6	156.3	172.6	124.7	94.3	78.6	70.4
21	Oberer Landschitzsee	138.6	90.0	52.3	73.7	111.4	85.1	129.4	124.2	162.1	189.5	115.7	89.3	92.8	60.6
22	Oberer Landwiersee	128.0	83.9	53.5	66.9	100.7	77.0	107.1	127.9	148.9	177.2	118.4	80.9	85.9	64.9
23	Oberer Schoenalmsee	119.2	73.2	40.2	48.9	92.4	70.5	100.5	117.5	139.5	174.7	107.1	63.2	84.9	51.1
24	Oberer Sonntagkarsee	139.6	93.1	64.5	84.7	99.7	83.5	110.8	145.4	162.5	175.5	133.0	102.7	81.3	77.8
25	Oberer Zwiefeldersee	147.1	92.4	49.3	77.1	99.2	90.4	132.5	138.7	170.1	179.1	131.2	100.1	88.4	63.9
26	Obersee	145.8	98.6	68.5	94.7	110.3	85.3	115.7	154.4	167.2	176.0	143.2	100.7	82.9	86.3
27	Pfannsee	138.6	93.4	66.4	90.5	105.3	80.6	108.9	146.9	160.1	169.0	134.2	94.3	78.1	81.9
28	Rantensee	142.0	90.3	51.3	76.7	106.6	83.9	132.3	127.3	166.5	188.1	118.7	92.6	89.0	61.5
29	Rauhenbergsee	132.1	86.3	58.8	76.3	93.9	77.6	105.5	135.4	155.3	171.6	124.0	93.3	77.9	69.7
30	Schwarzensee	158.4	98.0	52.8	84.1	100.9	96.6	135.5	155.6	184.1	182.3	149.4	103.9	85.5	73.4
31	Tiefenbachsee	124.1	75.7	41.5	51.6	96.9	74.0	103.2	124.7	144.3	182.9	111.8	65.0	83.6	53.3
32	Twenger Almsee	118.4	72.7	40.2	48.2	90.6	69.8	100.1	116.4	138.6	172.8	106.6	63.5	84.6	50.7
33	Unterer Giglachsee	133.1	85.3	57.7	70.6	98.1	78.0	104.7	137.2	157.5	180.1	124.5	85.5	80.9	68.1
34	Unterer Kaltenbachsee	143.7	87.4	45.3	68.8	88.2	86.4	125.3	138.4	167.3	171.9	132.6	97.9	80.6	61.7
35	Unterer Klaffersee	132.8	86.6	59.6	77.7	93.3	76.5	104.6	136.9	156.7	170.1	125.4	94.4	76.9	71.4
36	Unterer Klaffersee	159.9	100.6	54.4	86.2	106.5	97.7	135.5	159.2	185.0	184.7	154.4	106.3	87.8	76.8
37	Unterer Landschitzsee	128.1	82.5	48.7	65.6	98.8	77.4	116.0	117.9	150.2	178.0	111.3	82.7	84.9	57.1
38	Unterer Landwiersee	128.0	83.5	54.2	67.2	98.3	75.8	106.1	128.3	149.6	175.3	117.6	82.6	84.1	65.5
39	Unterer Sonntagkarsee	139.8	93.0	64.5	85.2	99.2	82.0	110.6	145.8	163.1	174.1	134.0	102.2	80.7	78.7
40	Unterer Wirpitschsee	121.0	74.2	40.6	49.4	93.1	71.3	101.9	119.8	141.4	177.4	109.7	64.4	84.9	52.3
41	Unterer Zwiefeldersee	145.7	89.6	46.9	73.2	93.6	87.3	128.5	138.7	169.9	177.0	131.0	98.7	83.8	63.4
42	Weissensee	159.8	99.6	53.1	86.3	105.1	97.8	134.8	159.5	185.0	184.6	153.5	104.3	85.8	75.5
43	Wildlochsee	147.1	99.7	69.3	96.1	111.6	87.3	116.9	156.0	168.4	178.5	143.3	102.3	83.8	86.5
44	Zwerfenbergsee	134.4	88.4	60.1	76.0	95.0	79.6	109.1	136.4	157.6	174.2	126.3	96.9	81.4	71.4

**Table A.5:** Average precipitation sums for the months JJA and the rest of the year, as well as average monthly precipitation sums for all catchments based on spatially interpolated data.

## B. Figures

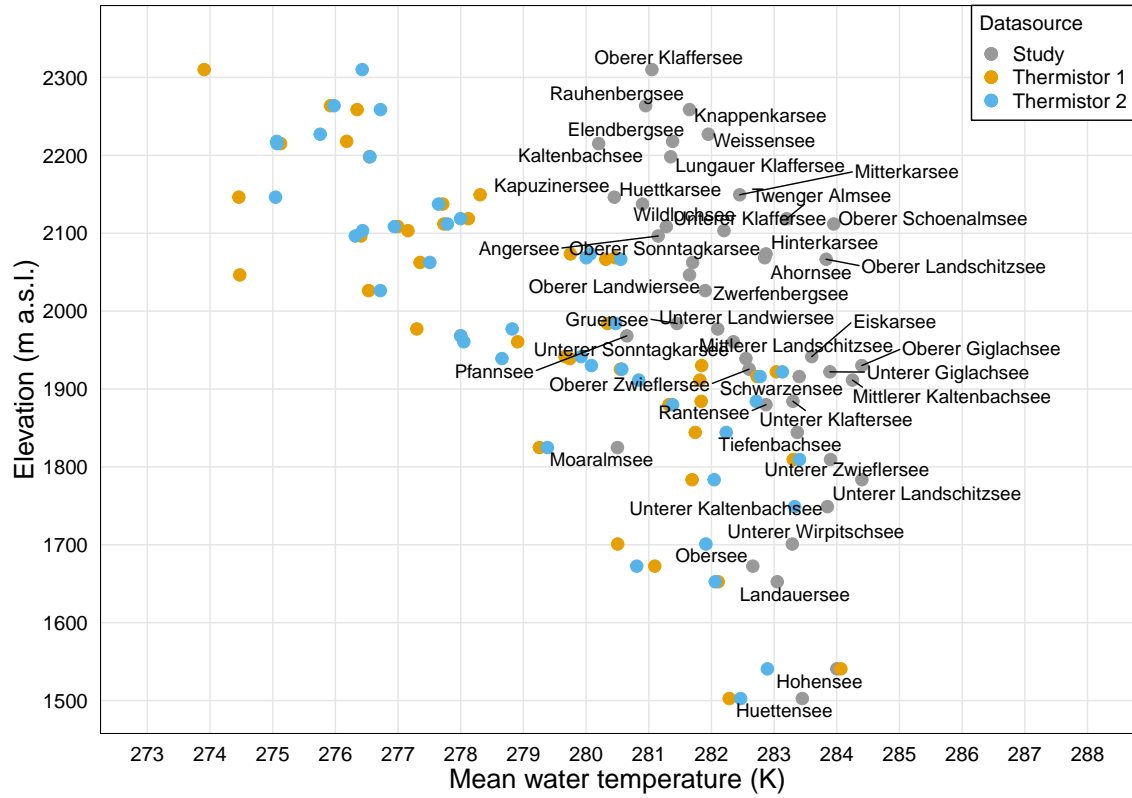


**Figure B.1:** Comparison of the summer water temperatures reported by the initial study and the mean values for the month of June calculated with the obtained raw data.

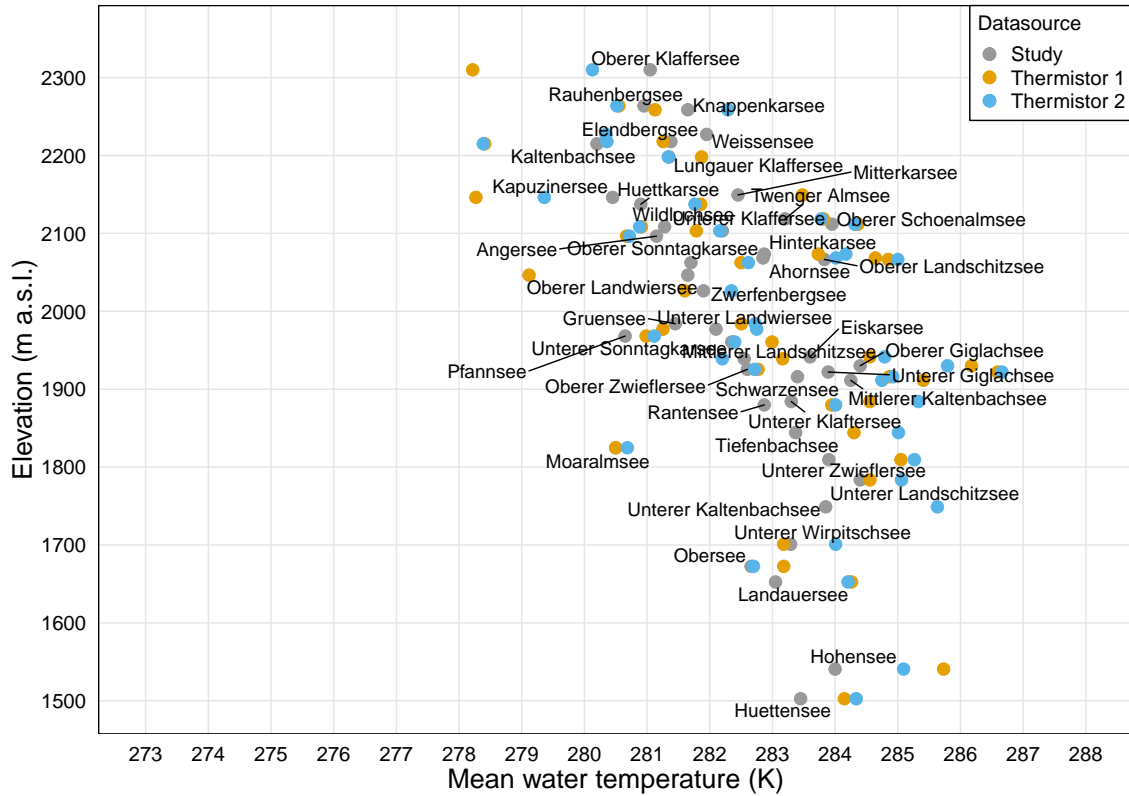


**Figure B.2:** Comparison of the summer water temperatures reported by the initial study and the mean values for the month of July calculated with the obtained raw data.

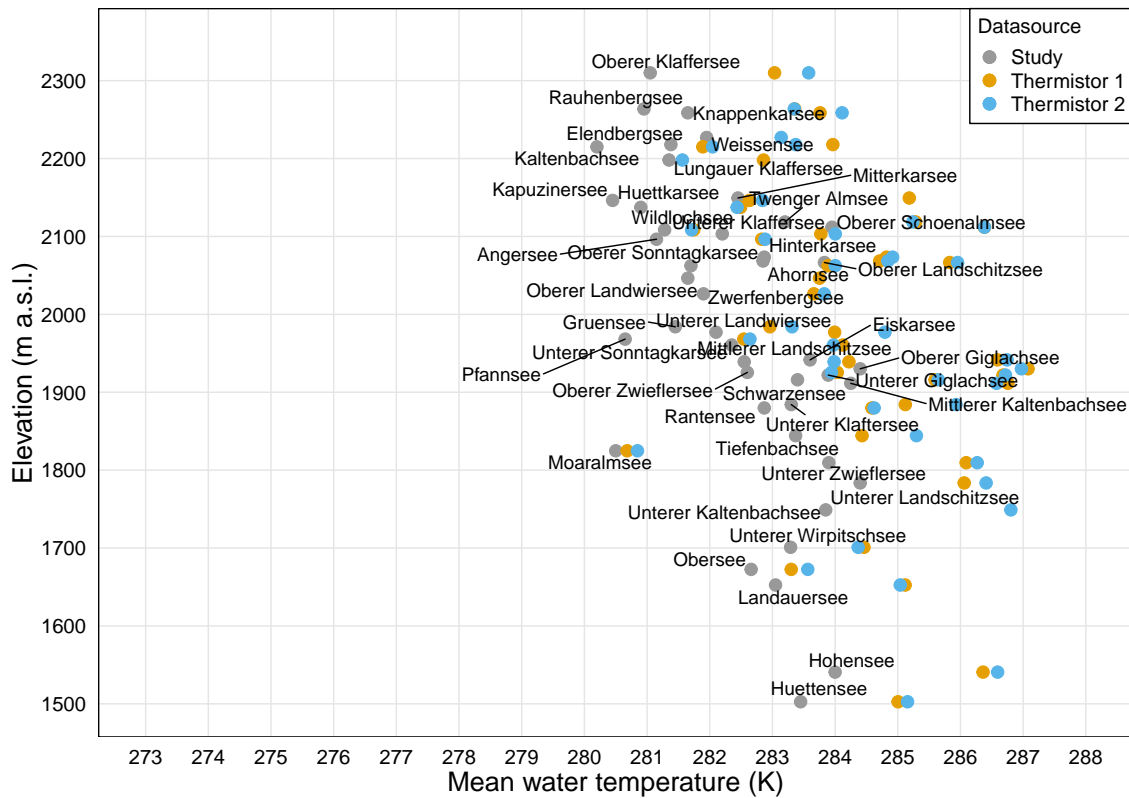


**Figure B.3:** Comparison of the summer water temperatures reported by the initial study and the mean values for the month of August calculated with the obtained raw data.

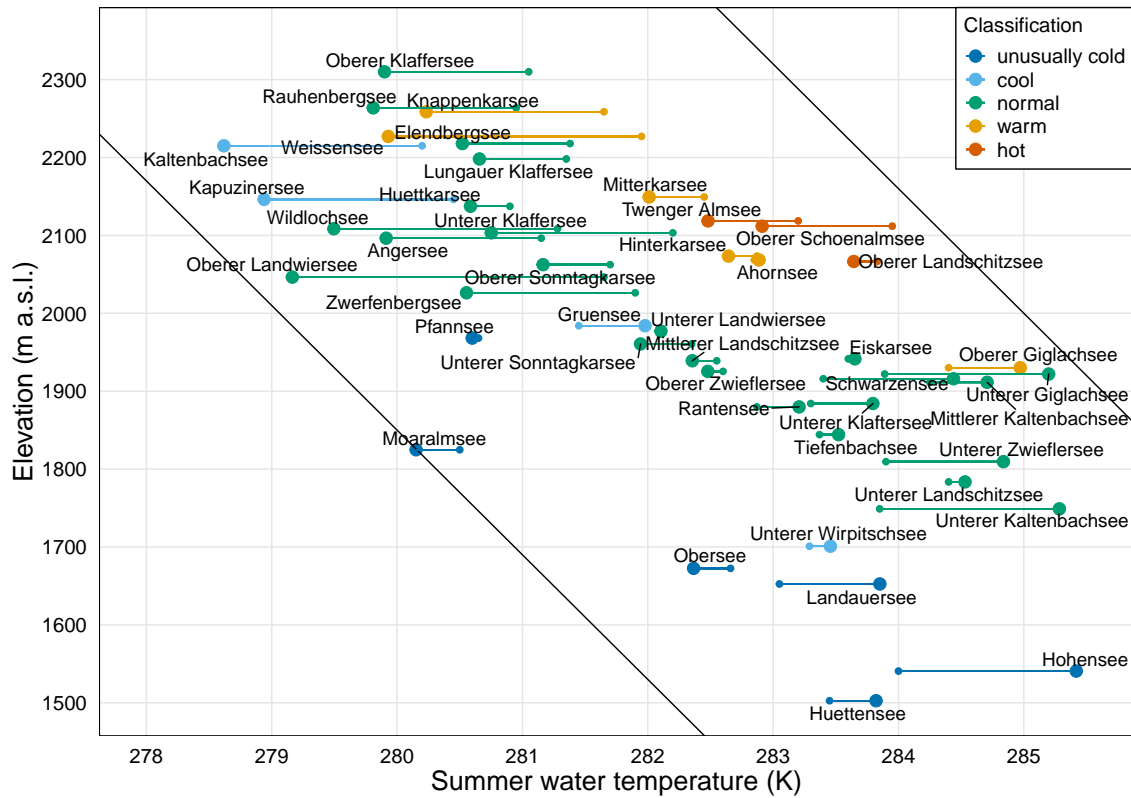


**Figure B.4:** Comparison of the plotted summer water temperature values of the initial study and the data provided for this master thesis.

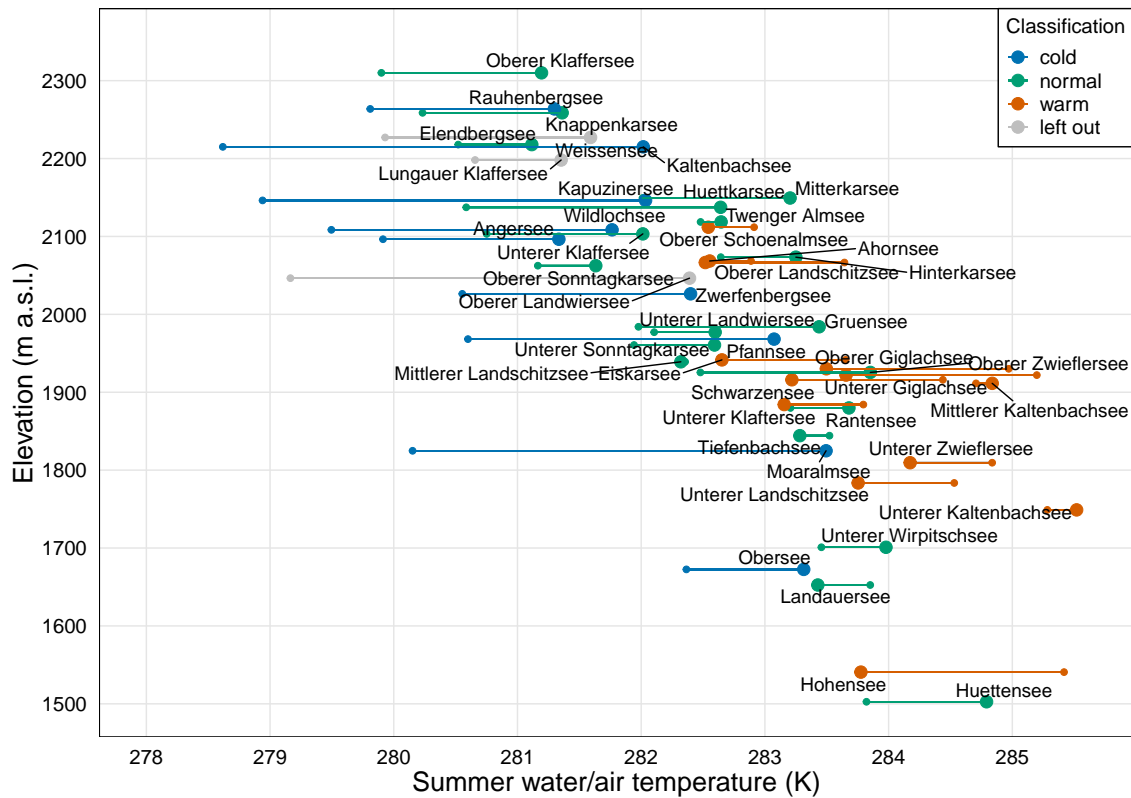


**Figure B.5:** Approach 2: Shifting of values from mean summer water temperature of the lake to mean summer air temperature of the catchment.